

“Speculative Influence Network” during financial bubbles: application to Chinese Stock Markets

L. Lin^{1,4*} and D. Sornette^{2,3†}

October 29, 2015

1. School of Business, East China University of Technology and Science, 200237 Shanghai, China
2. ETH Zurich, Department of Management, Technology and Economics, Scheuchzerstrasse 7, CH-8092 Zurich, Switzerland
3. Swiss Finance Institute, c/o University of Geneva, 40 blvd. Du Pont d’Arve, CH 1211 Geneva 4, Switzerland
4. Research Institute of Financial Engineering, East China University of Technology and Science, 200237 Shanghai, China

Abstract

We introduce the Speculative Influence Network (SIN) to decipher the causal relationships between sectors (and/or firms) during financial bubbles. The SIN is constructed in two steps. First, we develop a Hidden Markov Model (HMM) of regime-switching between a normal market phase represented by a geometric Brownian motion (GBM) and a bubble regime represented by the stochastic super-exponential Sornette-Andersen (2002) bubble model. The calibration of the HMM provides the probability at each time for a given security to be in the bubble regime. Conditional on two assets being qualified in the bubble regime, we then use the transfer entropy to quantify the influence of the returns of one asset i onto another asset j , from which we introduce the adjacency matrix of the SIN among securities. We apply our technology to the Chinese stock market during the period 2005-2008, during which a normal phase was followed by a spectacular bubble ending in a massive correction. We introduce the Net Speculative Influence Intensity (NSII) variable as the difference between the transfer entropies from i to j and from j to i , which is used in a series of rank ordered regressions to predict the maximum loss (%MaxLoss) endured during the crash. The sectors that influenced other sectors the most are found to have the largest losses. There is a clear prediction skill obtained by using the transfer entropy involving industrial sectors to explain the %MaxLoss of financial institutions but not vice versa. We also show that the bubble state variable calibrated on the Chinese market data corresponds well to the regimes when the market exhibits a strong price acceleration followed by clear change of price regimes. Our results suggest that SIN may contribute significant skill to the development of general linkage-based systemic risks measures and early warning metrics.

*Email: llin@ecust.edu.cn

†Email: dsornette@ethz.ch

1 Introduction

It is widely recognized that the backdrop of almost every preceding financial bubble is the prevalence of speculative mania, which causes valuation to drift out of whack, associated with a reinforcing imbalance between the size of unrealized supply and demand intentions, which forms the genesis of the potential market collapse. Speculative mania is by and large embodied in a variety of herding behaviors when investors imitate and follow other investors' strategies while tending to suppress their own private information and beliefs (Devenow and Welch, 1996; Avery and Zemsky, 1998). Such imitation can be either rational or irrational. Rational herding results from different possible mechanisms, such as (i) the anticipation by rational investors concerning noise trader's feedback strategies (Long et al., 1990), (ii) Ponzi schemes resulting from agency costs, (iii) monetary incentives given to competing fund managers (Dimitriadi, 2004; Dass et al., 2008) and (iv) rational imitation in the presence of uncertainty (Roehner and Sornette, 2000). In contrast, irrational herding is driven by market sentiment (Banerjee, 1992), fad (Bikhchandani et al., 1992), informational cascades (Barberis et al., 1998), 'word-of-mouth' effects from social imitation or influence (Shiller, 2000; Hong et al., 2005) or irrational positive feedback trading from extrapolation of past growth rate (Lakonishok et al., 1994; Nofsinger and Sias, 1999).

The challenge of diagnosing bubbles can thus be reduced to the detection and characterization of the regularities associated with herding effects in real time, with the goal of predicting the potential upcoming regime-shift and possible large sell-off resulting from their evolution. Most existing analyses have emphasized *herding of the overall market*, considering that investors tend to synchronize their behavior across the whole investment horizon. Accordingly, methods to detect bubbles have been focused mostly on representations of the whole market performance, in general by using market indices. The rationale is that, during bubble regimes when widespread speculative behavior is prevalent, individual stocks tend to become cross-sectionally more tightly correlated in their behavior and follow the general market dynamics. Notwithstanding this fact, the focus on market indices rather than the constituting individual stocks is bound to overlook endogenous structures of *herding within the universe of stocks* (see e.g. Sias (2004), Choi and Sias (2009)) and could potentially miss useful patterns associated with the dynamics of speculation during the bubble build up. In particular, the financial crisis of 2008 that followed a large bubble regime (Brunnermeier and Oehmke, 2013; Sornette and Cauwels, 2014) suggests that there is important information for the development of systemic risk metrics imbedded in the study of speculative bubble behavior in disaggregated industrial or firm level.

This paper presents an extension of more conventional bubble diagnosing methods by breaking down the structure of investment herding into its individual firm components. For this, we introduce the novel concept of the *Speculative Influence Network* (SIN), defined as a directional weighted network representing the causal speculative influencing relationships between all pairs of investment targets. In other words, we quantify how speculative trading in one asset may draw speculative trading in other asset. Here, we will focus on stocks, but the method is more generally applicable to any basket of assets. Specifically, we first estimate in real time the probability of speculative trading in each stock in the basket of interest, using a bubble identifying technique that was introduced for whole market indices but that we now extend to individual stocks. The strength of the bubble at the level of a single stock may increase or fade multiple times during the development of a global market bubble, perhaps due to particular idiosyncratic properties of the firm and of the corresponding industrial sector. The *Hidden Markov Modeling* (HMM) approach, which is specially designed to calibrate regime-switching processes, is thus a convenient methodology to make our bubble detection approach at the individual stock level more robust. Once we have characterized the subset of stocks being qualified in a bubble regime, we calculate the *Transfer Entropy* (TE), which is a measure developed in Information Science to quantify the casual relationship between variables. The underlying intuition behind this method is that, if a

stock Y exhibits a strong speculative influence on another stock X , then the existence of speculative trading of X can be predicated on the evidence of speculative trading on Y . In the language of Information Science, there is an information flow from Y towards X , which is quantified by the entropy transfer from Y to X .

The essential first step is of course to detect the presence of a bubble. For this, we borrow from the simple and generic prescription that a bubble is a transient regime characterized by faster-than-exponential (or super-exponential) growth (see e.g. (Hüsler et al., 2013; Kaizoji et al., 2015; Leiss et al., 2015; Sornette and Cauwels, 2015; Ardila-Alvarez et al., 2015) for recent empirical tests and models). The “super-exponential” behavior results from the existence of positive nonlinear feedback mechanisms, for instance of past price increases on future returns rises (Hüsler et al., 2013). Searching for transient super-exponential price behavior avoids the curse of other bubble detection methods that rely on the need to estimate a fundamental value in order to identify an abnormal pricing, the difference between the observed price and the supposed fundamental value being attributed to the bubble component. This avoids the critique of Gurkaynak (2008) in his study of the literature on rational bubbles and of econometric approaches applied to bubble detection, in which he reported that time-varying or regime-switching fundamentals could always be invoked to rationalize any declared bubble phenomenon. The second merit of super-exponential models is that they involve a mathematical formulation that inscribes the information on the end of the bubble, in the form of the critical time t_c at which the model becomes singular in the form of an a hyperbolic finite-time singularity (FTS). Actually, the bubble can end or burst before t_c , since, in the rational expectation bubble framework combined with the FTS models, t_c is just the most probable time of the bubble burst but not the only one because various effects can destabilize the price dynamics as time approaches t_c (such as drying of liquidity).

The existing literature that has contributed until now to the concept of super-exponential bubble can be divided into two classes: (a) bubbles with deterministic maximum termination time t_c and (b) bubbles with stochastic maximum termination time t_c . The first class takes its roots in the Johansen-Ledoit-Sornette (JLS) model (Johansen et al., 1999, 2000). Developed within the rational expectation framework, the JLS model translates the aggregate speculative behavior of investors into the existence of a critical dynamics associated with the self-organization of the system of mutually influencing traders. A parsimonious mathematical representation takes the form of the log-periodic power law singularity (LPPLS) dynamics. In addition to prices exhibiting a super-exponential acceleration, there is a long-term volatility that accelerates according to log-periodic oscillations embodying an accelerating cascade of exuberance followed by limited panics resuming into exuberance and so on. In this framework, the critical time t_c of the maximum duration of the bubble is also the most probable market crash time if it occurs. This critical time is treated as an intrinsic deterministic parameter in LPPLS bubble models. Since the introduction of the JLS model, there has been plenty of theoretical development of the LPPLS bubble framework, in particular expanding on the underlying mechanisms (Sornette, 1998; Sornette and Johansen, 1998; Ide and Sornette, 2002) and on model calibration (Zhou and Sornette, 2006a; Filimonov and Sornette, 2013; Lin et al., 2014). Concurrently, the LPPLS literature has developed empirically with both post-mortem studies of past bubbles as well as real-time ex-ante successful diagnostics of bubbles in a variety of financial markets, including western stock markets (Johansen et al., 1999; Johansen and Sornette, 2000; Sornette and Zhou, 2006), emerging stock markets (Johansen and Sornette, 2001; Giordano and Mannella, 2006; Zhou and Sornette, 2009; Cajueiro et al., 2009; Jiang et al., 2010), real-estate markets (Zhou and Sornette, 2006b, 2008), oil markets (Sornette et al., 2009), forex markets (Johansen et al., 1999; Matsushita et al., 2006) and so on.

Compared with LPPLS models, the other class of super-exponential bubble models, which explicitly consider the critical time t_c as an endogenous random variable depending on the market state and the investors’ aggregate expectations, have been much less explored. The Sornette-Andersen super-exponential bubble model serves as the first attempt in this field (Sornette and

Andersen, 2002; Andersen and Sornette, 2004). Under specific prescriptions of the nonlinear positive feedback effects, these bubble models have been proved to have their random critical times being distributed according to the inverse Gaussian distribution. Thereafter, the Sornette-Andersen model has been extended to richer situations in which the critical time satisfies an Ornstein-Uhlenbeck stochastic process (Lin and Sornette, 2013).

In this paper, we propose, in the first step of our investigations, to focus on the Sornette-Andersen super-exponential bubble model as the primary prescription to develop diagnostics of speculative trading, before developing in a second step the analysis of the structure of mutual interactions between stocks. First, the Sornette-Andersen model has an elegant analytical solution and enjoys a more straightforward representation of speculative trading. Second, it is more tractable within an integrated stochastic framework and allows for a natural and transparent implementation of the HMM approach, in which additional characteristics of speculation can be added. A first addition can be the condition of the stationarity of the critical end time due to the lack of synchronization. A second addition is the ingredient of log-periodicity of the long term volatility due to the interplay between the inertia of transforming information into decision in the presence of nonlinear momentum and price-reversal trading styles (Ide and Sornette, 2002).

In order to demonstrate the usefulness of our proposed speculative influence network (SIN), we perform our empirical study on the Chinese stock market. As an emerging financial market, the Chinese market has exhibited a number of dramatic bubbles and crashes (Jiang et al., 2010; Sornette et al., 2015), reflecting strong herding activities developing in a more opaque information environment with less regulatory control than mature western markets (Piotroski and Wong, 2011). A few previous works have revealed the existence of powerful speculative investors manipulating the market with relative facility, like in the so-called “pump and dump” strategy (Khawaja and Mian, 2005; Zhou et al., 2005; He and Su, 2009). Additionally, less-informed small and medium size Chinese investors have been shown to be prone to trend-chasing speculation (Li et al., 2009). Moreover, empirical studies suggest an acute tendency of herding among Chinese investors (Tan et al., 2008; Chiang et al., 2010), especially for institutional investors whose herding is found to play a role in destabilizing the whole market (Xu et al., 2013). From mid-2005, the two major stock indices of the Chinese stock market, i.e., the Shanghai Stock Exchange Composite (SSEC) index and the Shenzhen Stock Component (SZSC) index, rose six-fold in just two years. This extreme growth was then followed by a dramatic drop of about two-third of their peak values over a year. Though the transient prosperity of the financial market has been fueled by many compelling growth stories concerning the rapid fundamental growth of the Chinese economy, the roller-coaster performance of the whole market over the year of 2008 in particular offered hind-sights about the existence of a bubble with a mixture of herding, over-optimistic speculation and positive feedback trading (Jiang et al., 2010; Lin et al., 2014).

Our present study focuses on the Chinese stock market episodes from 2006 to 2008. To test the predictability of large cumulative losses associated with financial sell-offs in the Chinese stock market, we construct the SIN from 2006 to the end of 2007 when the market was still in a bullish state. We then search for possible early-warning signals in the percentage maximum loss (%MaxLoss) of each stock during 2008, using measures derived from the network-based analysis. The network is constructed by using the representative stocks portfolios and indices of various industrial sectors. Also, considering the implications to measure systemic risks, we expand the single node representing the financial sector in the original network to become a full sub-network made of all stocks from the financial sector, including banks, trust companies, securities firms and insurance companies. Our main empirical findings is that the total net influence effect measured with the Transfer Entropy (TE) method in industrial sectors (except for the financial sector and for financial institutions) is a significant determinant of the %MaxLoss of a number of stocks. Moreover, the gross TE to all industrial sectors significantly explains the %MaxLoss of financial institutions, whereas the total TE to or from financial institutions are not good explanatory indi-

cators to predict the %MaxLoss of non-financial sectors. These results suggest that the SIN can not only be used to construct a cross-sectional anatomy of bubbles but can also help in complementing the analytics of linkage-based systemic risk measures, by estimating the interconnection of institutions with respect to their vulnerability to exuberant speculation.

The structure of this article is as follows. Section 2 first introduces the Sornette-Andersen super-exponential bubble model with stochastic termination times and then discusses the detectability of speculative trading using the HMM approach from the regime-switching perspective of bubble onset and burst. In Section 3, we investigate how to build the speculative influence network (SIN) for a financial market with the help of the Transfer Entropy between stocks. Section 4 studies the practical relevance of the SIN and also explores possible measures of systemic risks that can be derived from it. An empirical application is made to the Chinese stock market. Finally, we conclude and sketch out potential extensions in Section 5.

2 Regime-Switching speculative bubbles with super exponential growth

2.1 The Sornette-Andersen bubble model

According to the principle underlying the whole analysis of this paper, speculative trading during a bubble is characterized by positive feedbacks, i.e., the higher the number of interested investors and the higher the price, the larger the increase of new stock purchases and the higher the price growth. Positive feedbacks are contributed by a large diversity of herding activities, leading to copycats rushing to follow their leaders (Chincarini, 2012). It is worth noting that, while herding has been largely documented to be a trait of noise traders, it is actually rational for bounded rational agents to also enter into social imitation, because the collective behavior may reveal information otherwise hidden to the agents. Moreover, even in the absence of information, it may also be rational to imitate one's social network because it may reflect the consensus who decisions are incorporated in subsequent returns (Roehner and Sornette, 2000).

Once positive feedback takes over, the financial market, like all systems with positive feedback, enters a state of increasing unbalance, with unsustainable increasing rates of return. Positive feedbacks lead to faster-than-exponential price appreciation: as prices increase, the expectation of future growth increases even further, pushing anticipation of future returns upwards. This means that the growth rate grows itself. As a constant growth rate of the price (namely, a constant return) corresponds to an exponential price trajectory, a growing growth rate leads (in many specifications) to a faster-than-exponential price path with a finite-time singularity signaling the end of the bubble. The technical analysis literature casually refers to this pattern as “parabolic” or “hyperbolic” growth because of the corresponding upward curvature (convexity) of the log-price as a function of time. The important point for our purpose is that the transient faster-than-exponential price path provides a diagnostic of speculative bubbles that is fundamentally different from the standard academic methods that emphasize more the detection of just abnormal exponential growth regimes above the fundamental price or of mildly explosive regimes. One could term the regimes we refer to as being “super-explosive”, to emphasize the difference with the term “explosive” often attributed to an exponential regime (which is the norm in finance and in economics, as well as in demographics, because an exponential growth just reflects the mechanism of proportional growth, which is nothing but compounding interest in finance).

In the context of speculative bubbles, the Sornette-Andersen model is arguably the most parsimonious representation to capture a transient “super-explosive” signature in a continuous stochastic framework, which formulates the interplay between multiplicative noise and nonlinear positive feedbacks onto future returns and volatility. According to the model, the price dynamics in the

bubble regime is assumed to be described by the following stochastic differential equation (Sornette and Andersen, 2002):

$$\frac{dp}{p} = [\mu_1(p) + \mu_2(p)]dt + \sigma(p)dW - \kappa dj \quad (1)$$

where the first drift term $\mu_1(p) = \mu p^n$, $n > 0$ represents the nonlinear positive feedback effect that larger asset price feeds a larger growth rate (Hüsler et al., 2013), which leads to even larger price and so on. The parameters μ and n are respectively the effective drift coefficient and strength of nonlinear positive feedback effects. The diffusion part is specified by $\sigma(p) = \sigma p^n$, $n > 0$, with the same strength of the nonlinear positive feedbacks of price, and can be interpreted as a conditional nonlinear heteroskedasticity. Intuitively, the term may be rationalized by the prevalence of hedging strategies using general Black-Scholes option models and of other herding behaviors discussed before. The parameter σ denotes the magnitude of the stochastic component, which sets the scale of volatility. The last term $-\kappa dj$ represents the crash, where $dj = 1$ when the crash occurs and $dj = 0$ otherwise, and κ is the crash amplitude. The crash hazard rate $h(t) := E[dj]$ (where $E[\cdot]$ is the expectation operator) is specified by the condition of no arbitrage, which translates into the fact that the price is a Martingale: $E[\frac{dp}{p}] = 0$. This leads to

$$h(t) = \frac{1}{\kappa}(\mu_1(p) + \mu_2(p)) . \quad (2)$$

Without the drift term $\mu_2(p)$ and neglecting the crashes, expression (1) transforms into the standard Stratonovich deterministic equation,

$$\frac{dp}{p} = (\mu dt + \sigma dW)p^n, \quad n > 0 \quad (3)$$

giving the intuitive interpretation that the market noise dW gradually accumulates in the price through a simple multiplicative mechanism reinforced by the nonlinear term p^n .

The second drift term is set to be $\mu_2(p) = \frac{n+1}{2}\sigma^2(p)$. As the market required a risk premium for the existing volatility and upcoming crash, this term serves to balance the subtle interplay between multiplicative noise and nonlinear positive feedbacks. With this additional convenient device, Itô calculation of these stochastic differential equations (1) can be drastically simplified, as we will see soon.

The most striking feature of the model is that the nonlinearity ($n > 0$) creates a singularity in finite time and the multiplicative noise makes it stochastic. To see this, let us first consider the case $\sigma \rightarrow 0$ and $\kappa \rightarrow 0$, for which eq.(1) reduces to the deterministic price dynamics $\frac{dp}{p} = \mu p^n dt$, whose solution reads

$$p(t) = (n\mu)^{-\frac{1}{n}} [t_c - t]^{-\frac{1}{n}}, \quad t_c = \frac{p_0^{-n}}{n\mu} \quad (4)$$

where $p_0 = p(t = t_0)$. Note that such deterministic dynamics is characterized by a fixed critical time, t_c , such that $p(t)$ diverges when time approaches t_c from below. This critical time is called a movable singularity, because it depends on the initial condition p_0 in addition to the parameters of the model. Reintroducing a non-zero volatility, and conditional on the absence of a crash ($dj = 0$), Itô calculus applied to (1) provides the following explicit analytical solution (See Sornette and Andersen (2002) for the complete derivation therein):

$$p(t) = [n\mu(t_c - t) - n\sigma W_t]^{-\frac{1}{n}}, \quad t_c = \frac{p_0^{-n}}{n\mu} \quad (5)$$

This solution recovers, as it should, the deterministic solution (4) for $\sigma = 0$. The price now exhibits a stochastic behavior, which can still diverge when there is a time such that the denominator

$n\mu(t_c - t) - n\sigma W_t$ crosses 0. At $t = 0$, the denominator starts from an initial positive value $n\mu t_c$. In the presence of the negative drift $-n\mu t$ and notwithstanding the presence of the Wiener process, the denominator will cross 0 with probability 1. The corresponding stochastic critical time \tilde{t}_c at which the price diverges is thus controlled by a first-passage problem when the drifting random walk motion $n\mu t + n\sigma W_t$ first encounters the value $n\mu t_c = p_0^{-n}$. From standard results of first-passage problems (Redner, 2001; Jeanblanc et al., 2009), the stochastic critical time \tilde{t}_c is found to be distributed according to the *Inverse Gaussian* distribution

$$\tilde{t}_c \sim \mathcal{IG} \left(\frac{p_0^{-n}}{n\mu}, \left[\frac{p_0^{-n}}{n\sigma} \right]^2 \right). \quad (6)$$

In fact, with the specification (1) augmented by (2), the price never diverges. This is because, as the price accelerates, so does even more its instantaneous growth rate $\mu_1(p) + \mu_2(p)$ and therefore so does the crash hazard rate via expression (2). This is aimed at embodying the fact that the bubble collapses as a result of the ebb of speculation and withdrawal of intended demand when an unsustainable state is becoming more obvious or due to increasing scarcity of money and credit. In other words, a crash always occurs before the price goes too high, ensuring long-term stationarity (Sornette and Andersen, 2002).

Note that the price dynamics (5) reduces to the geometric random walk when the strength of positive feedback vanishes ($n = 0$):

$$\lim_{n \rightarrow 0} p(t) = p_0 \cdot \lim_{n \rightarrow 0} [1 - n(\mu t + \sigma W_t)]^{-\frac{1}{n}} = p_0 e^{\mu t + \sigma W_t}, \quad (7)$$

which is indeed the solution of the standard Black-Scholes framework obtained as the limit $n \rightarrow 0$ of equation (1) (with $\kappa = 0$).

2.2 Hidden Markov modelling (HMM) calibration approach

We propose to extend the Sornette-Andersen model summarized in the previous section by combining it with a standard geometric random walk, supposed to represent the normal regime of markets. The complete price process is then described by regime switching between the dynamics described by the Sornette-Andersen model with significantly positive value of n and the degenerated geometric random walk for $n = 0$. Then, the existence of speculative trading can be judged by estimating the probability that the market is in bubble state ($n > 0$) or in the normal state ($n = 0$). For this, we convert the bubble model into a Hidden Markov modeling (HMM) framework and then calibrate all parameters in the model to identify the onsets and ends of bubbles, following a procedure that we now describe. Because crashes represented by the jump term dj in (1) as rare, we chose to not identify them and only rely on the structural differences between the process conditional on no crash for $n > 0$ and $n = 0$.

For the sake of conciseness and efficiency of the presentation, in the following discussion, we introduce a novel mathematical representation of probability distribution functions and of conditional density functions. They resemble the famous “bra-ket” notations in Dirac notations in Quantum Mechanics. To be clear, no new results are derived, it is just a notation used for its compactness and coherence. The notations are as follows. We use “bra” to denote the probability density for a random variable, i.e., $\langle x | := f_{\tilde{x}}(x)$; We use “ket” to denote the “conditional on” operation. Formal “multiplication” of a bra-vector and a ket vector gives the conditional density, i.e., $\langle x | \cdot | y \rangle = \langle x | y \rangle := f_{\tilde{x}|\tilde{y}}(x|y)$. In the Appendix A, we show that, with the addition of a few formal transformation rules, more complicated expressions can be nicely represented, such as the decomposed conditional joint density or Bayesian formulas for multivariate conditional densities. This is convenient to present the derivation of the formulas of our proposed HMM

procedure developed to estimate the super-exponential Sornette-Andersen bubble model from the perspective of a state-dependent regime-switching process.

In order to formulate the HMM, we assume there is an underlying stochastic state process s_t that indicates the prevalence of speculative trading, which is unobserved by the investors. The state is switching between 0 and 1, signalling respectively the “normal” and bubble states. We use

$$q_{ij} = \langle s_t = j \mid s_{t-1} = i \rangle, \quad i, j = 0, 1 \quad (8)$$

to denote the element (i, j) of the Markov-chain transition probability matrix.

Two cases must be considered in the absence of switching, whose specifications derive straightforwardly from the definition of the Sornette-Andersen model:

- $(s_t, s_{t-1}) = (0, 0)$: The market remains in the state without bubble. Therefore, the price dynamics p_t follows the geometric Brownian motion, i.e., $y_t \mid y_{t-1} \sim \mathcal{N}(\mu_0 + y_{t-1}, \sigma_0^2)$, where $y_t = \ln p_t$. Specifically, the transition probability for y_t is expressed as

$$\ln \langle y_t \mid s_t = 0, s_{t-1} = 0, y_{t-1} \rangle = -\frac{1}{2} \ln 2\pi - \ln \sigma_0 - \frac{1}{2} \cdot \left(\frac{y_t - y_{t-1} - \mu_0}{\sigma_0} \right)^2. \quad (9)$$

- $(s_t, s_{t-1}) = (1, 1)$: The market is experiencing a continuing super-exponential bubble characterized by the prevalence of speculation and herding associated with positive feedback. Hence, the price dynamics p_t is captured by the Sornette-Andersen model summarized by eq.(5) in the absence of crash. The corresponding discrete formulation, $p_t^{-n} \mid p_{t-1}^{-n} \sim \mathcal{N}(p_{t-1}^{-n} - n\mu_1, n^2\sigma_1^2)$ leads to the transition probability for y_t (See Appendix B for the detailed proof) given by

$$\ln \langle y_t \mid s_t = 1, s_{t-1} = 1, y_{t-1} \rangle = -\frac{1}{2} \ln 2\pi - \ln n\sigma_1 - \frac{1}{2} \cdot \left(\frac{e^{-ny_t} - e^{-ny_{t-1}} + n\mu_1}{n\sigma_1} \right)^2 + \ln n - ny_t. \quad (10)$$

In the presence of a regime switch, we have to make some additional assumption and we choose the simplest possible one:

$$\begin{cases} \langle y_t \mid s_t = 0, s_{t-1} = 1, y_{t-1} \rangle = \left| \frac{1}{\mu_0} \right| \cdot \mathbf{1}_{\{-\kappa \leq y_t < y_{t-1}\}} & (11) \\ \langle y_t \mid s_t = 1, s_{t-1} = 0, y_{t-1} \rangle = \left| \frac{1}{\mu_1} \right| \cdot \mathbf{1}_{\{y_{t-1} \leq y_t \leq \kappa\}}, & (12) \end{cases}$$

where $\mathbf{1}_{\{\text{condition}\}}$ is the indicator function that equals to 1 when condition is met, otherwise it gives 0. Expression (11) writes that, at the time when a bubble ends, the price drops by an amount that is bounded by the crash amplitude κ . Similarly, expression (12) expresses that, a bubble starts, the price tends to appreciate. We bound the maximum amplitude of appreciation by the scale set by κ . The simplicity of (11) and (12) allows for an analytical expression of the likelihood function, which is convenient for its maximisation and determination of the model parameters, as we shall see below.

The price dynamics of our state-dependent Markov-switching periodically collapsing bubble model is entirely encoded in the vector of parameters $\boldsymbol{\theta} = (\mu_0, \sigma_0, \mu_1, \sigma_1, n, q_{00}, q_{11}, q_{01}, q_{10})$. Because the underlying state variable s_t is hidden, it is natural to apply the *Expectation-Maximization (EM)* algorithm to estimate $\boldsymbol{\theta}$ (Dempster et al., 1977; Kim and Nelson, 1999). In a nutshell, the EM algorithm is implemented by iteratively performing two steps until meeting the convergence condition : (1) calculation of the expectation of the log-likelihood evaluated using the current parameters estimates (called E-step) and (2) maximization of the obtained averaged log-likelihood

function to obtain the optimized posterior estimates (called M-step). Applied to our model, the E-step reads

$$\ln \mathcal{L}_{\theta|\theta^{(k-1)}} = \sum_{1 \dots T} \left(\ln \langle y_{-\infty}^T, s_{-\infty}^T | \theta \rangle \langle y_{-\infty}^T, s_{-\infty}^T | \theta^{(k-1)} \right) \quad (13)$$

where the notation $\cdot_{-\infty}^T$ means that the corresponding variable is multidimensional and covers all the time steps from the start 0 to the end T of the time window. The symbol $\sum_{1 \dots T}$ means that the summation over all states $s_t, t = 1, \dots, T$ is performed. The above expectation step (13) can be expanded into (See Appendix C.1 for the detailed derivation)

$$\ln \mathcal{L}_{\theta^{(k)}|\theta^{(k-1)}} = \langle y_{-\infty}^T | \theta^{(k-1)} \cdot \left(\sum_{t=1}^T \sum_{\substack{s_t=1,0 \\ s_{t-1}=1,0}} \left(\ln \langle y_t | s_t, s_{t-1}, y_{t-1} \rangle_{\theta^{(k)}} + \ln \langle s_t | s_{t-1} \rangle_{\theta^{(k)}} \right) \langle s_{t-1}, s_t | y_{-\infty}^T \rangle_{\theta^{(k-1)}} \right) \quad (14)$$

In the M-step (See Appendix C.2, C.3 and C.4), we then obtain the following expressions for the corresponding posterior estimates of the parameters:

- $\mu_0^{(k)} = \frac{\sum_{t=1}^T \omega_{(0,0);t}^{(k-1)} (y_t - y_{t-1})}{\sum_{t=1}^T \omega_{(0,0);t}^{(k-1)}}, \quad \omega_{(0,0);t}^{(k-1)} := \langle s_t = 0, s_{t-1} = 0 | y_{-\infty}^T \rangle_{\theta^{(k-1)}}$
- $\sigma_0^{(k)} = \sqrt{\frac{\sum_{t=1}^T \omega_{(0,0);t}^{(k-1)} (y_t - y_{t-1} - \mu_0^{(k)})^2}{\sum_{t=1}^T \omega_{(0,0);t}^{(k-1)}}}, \quad \omega_{(0,0);t}^{(k-1)} := \langle s_t = 0, s_{t-1} = 0 | y_{-\infty}^T \rangle_{\theta^{(k-1)}}$
- $\mu_1^{(k)} = \frac{\sum_{t=1}^T \omega_{(1,1);t}^{(k-1)} (p_{t-1}^{-n} - p_t^{-n})}{n \sum_{t=1}^T \omega_{(1,1);t}^{(k-1)}}, \quad \omega_{(1,1);t}^{(k-1)} := \langle s_t = 1, s_{t-1} = 1 | y_{-\infty}^T \rangle_{\theta^{(k-1)}}$
- $\sigma_1^{(k)} = \sqrt{\frac{\sum_{t=1}^T \omega_{(1,1);t}^{(k-1)} (p_t^{-n} - p_{t-1}^{-n} + n\mu_1^{(k)})^2}{n^2 \sum_{t=1}^T \omega_{(1,1);t}^{(k-1)}}}, \quad \omega_{(1,1);t}^{(k-1)} := \langle s_t = 1, s_{t-1} = 1 | y_{-\infty}^T \rangle_{\theta^{(k-1)}}$
- The value $n^{(k)}$ is solution of the following nonlinear univariate equation

$$\sum_{t=1}^T \left(-\frac{(p_t^{-n} - p_{t-1}^{-n} + n\mu_1)(-p_t^{-n} \ln p_t + p_{t-1}^{-n} \ln p_{t-1} + \mu_1)}{n^2 \sigma_1^2} + \frac{1}{n} - \ln p_t \right) \omega_{(1,1);t}^{(k-1)} = 0 \quad (15)$$

- $q_{ij}^{(k)} = \frac{\sum_{t=1}^T \langle s_t = j, s_{t-1} = i | y_{-\infty}^T \rangle_{\theta^{(k-1)}}}{\sum_{t=1}^T \langle s_{t-1} = i | y_{-\infty}^T \rangle_{\theta^{(k-1)}}}, \quad i, j = 0, 1$

In order to use these expressions, we need to have the values of $\omega_{(0,0);t}^{(k-1)}$ and $\omega_{(1,1);t}^{(k-1)}$, which requires to determine $\langle s_t, s_{t-1} | y_{-\infty}^T \rangle$ and $\langle s_t | y_{-\infty}^T \rangle$. For this, we first adopt a Hamilton filtering procedure (see (Hamilton, 1989)) to obtain $\langle s_t | y_{-\infty}^t \rangle, 0 \leq t \leq T$, which can be decomposed in three steps:

1. *Prediction Step:* from $\langle s_{t-1} | y_{-\infty}^{t-1} \rangle$ to $\langle s_t, s_{t-1} | y_{-\infty}^{t-1} \rangle$

$$\begin{aligned} \langle s_t, s_{t-1} | y_{-\infty}^{t-1} \rangle &= \langle s_t, s_{t-1} | \cdot | y_{-\infty}^{t-1} \rangle = (\langle s_t | s_{t-1} \rangle \langle s_{t-1} | \cdot \rangle | y_{-\infty}^{t-1} \rangle) = \langle s_t | s_{t-1}, y_{-\infty}^{t-1} \rangle \langle s_{t-1} | y_{-\infty}^{t-1} \rangle \\ &= \langle s_t | s_{t-1} \rangle \langle s_{t-1} | y_{-\infty}^{t-1} \rangle \end{aligned} \quad (16)$$

This is nothing but the composed conditional joint density (See Appendix A).

2. *Updating Step*: from $\langle s_t, s_{t-1} | y_{-o}^{t-1} \rangle$ to $\langle s_t, s_{t-1} | y_{-o}^t \rangle$

$$\langle s_t, s_{t-1} | y_{-o}^t \rangle = \langle s_t, s_{t-1} | y_{-o}^{t-1}, y_t \rangle = \langle s_t, s_{t-1} | y_{-o}^{t-1} \rangle \frac{\langle y_t | s_t, s_{t-1}, y_{-o}^{t-1} \rangle}{\langle y_t | y_{-o}^{t-1} \rangle} \quad (17)$$

$$= \frac{\langle y_t | s_t, s_{t-1}, y_{-o}^{t-1} \rangle \langle s_t, s_{t-1} | y_{-o}^{t-1} \rangle}{\sum_{t-1, t} \langle y_t | s_t, s_{t-1}, y_{-o}^{t-1} \rangle \langle s_t, s_{t-1} | y_{-o}^{t-1} \rangle} \quad (18)$$

The validity of eq. (17) is based on the multivariate Bayesian formula (See Appendix A for details).

3. *Summation Step*: from $\langle s_t, s_{t-1} | y_{-o}^t \rangle$ to $\langle s_t | y_{-o}^t \rangle$

$$\begin{aligned} \langle s_t | y_{-o}^t \rangle &= \langle s_t | \cdot \left(\sum_{t-1} |s_{t-1} \rangle \langle s_{t-1} | \right) | y_{-o}^t \rangle = \left(\sum_{t-1} \langle s_t | s_{t-1} \rangle \langle s_{t-1} | \right) | y_{-o}^t \rangle = \left(\sum_{t-1} \langle s_t, s_{t-1} | \right) | y_{-o}^t \rangle \\ &= \sum_{t-1} \langle s_t, s_{t-1} | y_{-o}^t \rangle \end{aligned} \quad (19)$$

This provides the *filtering probability* $\langle s_t | y_{-o}^t \rangle$, which quantifies the probability for a given bubble state to be present, based on the current available market information.

Second, with the obtained filtering probability, we take advantage of a backward smoothing approach to estimate $\langle s_t, s_{t-1} | y_{-o}^T \rangle$ and $\langle s_t | y_{-o}^T \rangle$, which is inspired by Kim's smoothing routine (See Kim and Nelson (1999) for a discussion therein). Let y_{t+1}^- denote all of the remaining log-prices $\ln(p_t)$ expressed at time following time t in the observation window from 1 to T , i.e., $y_{-o}^T = \{y_{-o}^t, y_{t+1}^-\}$. The backward prediction is then expressed as

$$\langle s_{t+1}, s_t | y_{-o}^T \rangle = \langle s_t | s_{t+1}, y_{-o}^T \rangle \langle s_{t+1} | y_{-o}^T \rangle = \langle s_t | s_{t+1}, y_{-o}^t, y_{t+1}^- \rangle \langle s_{t+1} | y_{-o}^T \rangle \quad (20)$$

$$= \langle s_t | s_{t+1}, y_{-o}^t \rangle \langle s_{t+1} | y_{-o}^T \rangle = \langle s_t | y_{-o}^t \rangle \frac{\langle s_{t+1} | s_t, y_{-o}^t \rangle}{\langle s_{t+1} | y_{-o}^t \rangle} \langle s_{t+1} | y_{-o}^T \rangle \quad (21)$$

$$= \langle s_t | y_{-o}^t \rangle \langle s_{t+1} | y_{-o}^T \rangle \frac{\langle s_{t+1} | s_t \rangle}{\sum_t \langle s_{t+1} | s_t \rangle \langle s_t | y_{-o}^T \rangle}. \quad (22)$$

The derivation of the r.h.s. in (21) is based on the multivariate Bayesian formula (See Appendix A). The detailed derivation from (20) to (21) can be found in Appendix C.5. This finally leads to the following expression to calculate $\langle s_t | y_{-o}^T \rangle$, which can be called *smoothing probability*:

$$\langle s_t | y_{-o}^T \rangle = \sum_{t+1} \langle s_t | s_{t+1} \rangle \langle s_{t+1} | y_{-o}^T \rangle = \sum_{t+1} \langle s_{t+1}, s_t | y_{-o}^T \rangle, \quad t = 1, \dots, T-1. \quad (23)$$

As its mathematical denotation to indicate, the *smoothing probability* $\langle s_t | y_{-o}^T \rangle$ measures the likelihood of the existence of bubbles in a given time interval by including the information of future prices. For our purpose of diagnosing a bubble and its possible dangerous time period for a burst, it is necessary to use the causal *filtering probability* $\langle s_t | y_{-o}^t \rangle$ and not the non-causal *smoothing probability* $\langle s_t | y_{-o}^T \rangle$. The later can however be useful for parameter estimations, which themselves impact on bubble detection.

2.3 Empirical estimation of the bubble probability in 16 financial markets

Figs. 1 and 2 show the estimated daily smoothing probability for the presence of super-explosive bubbles based on the HMM procedure in sixteen different global financial markets, represented by their major stock indices. Correspondingly, Figs. 3 and 4 display the estimated daily filtering

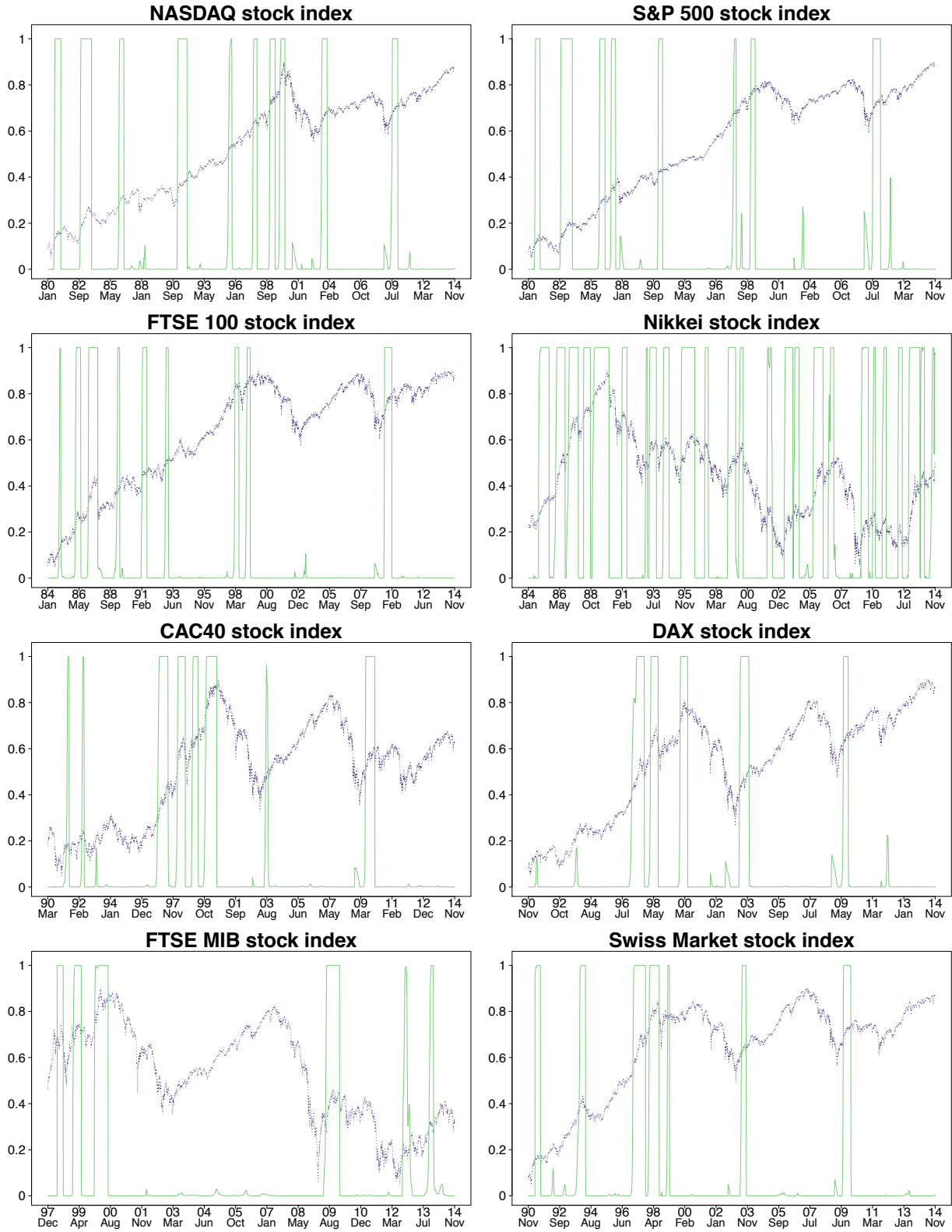


Figure 1: Estimated daily smoothing probabilities $\langle s_t | y_{-\infty}^T \rangle$ of the periodical collapsing super-exponential growth bubble embedded in the Hidden Markov Modeling (HMM) procedure represented with the palegreen thin continuous curve bouncing between 0 and 1 for eight stock exchanges: U.S. (Nasdaq and S&P500), U.K., Japan, France, Germany, Italy and Switzerland. All indices are given in logarithmic scale and are rescaled into $[0,1]$ for comparison. In order to mitigate the effects of identifying regime-shift too often as a result of daily price volatility, all indices are geometrically averaged over 100 days according to $\ln p_t^{\text{filtered}} = (1/100) \sum_{i=0}^{99} \ln p_{t-i}$, before implementing the EM algorithm.

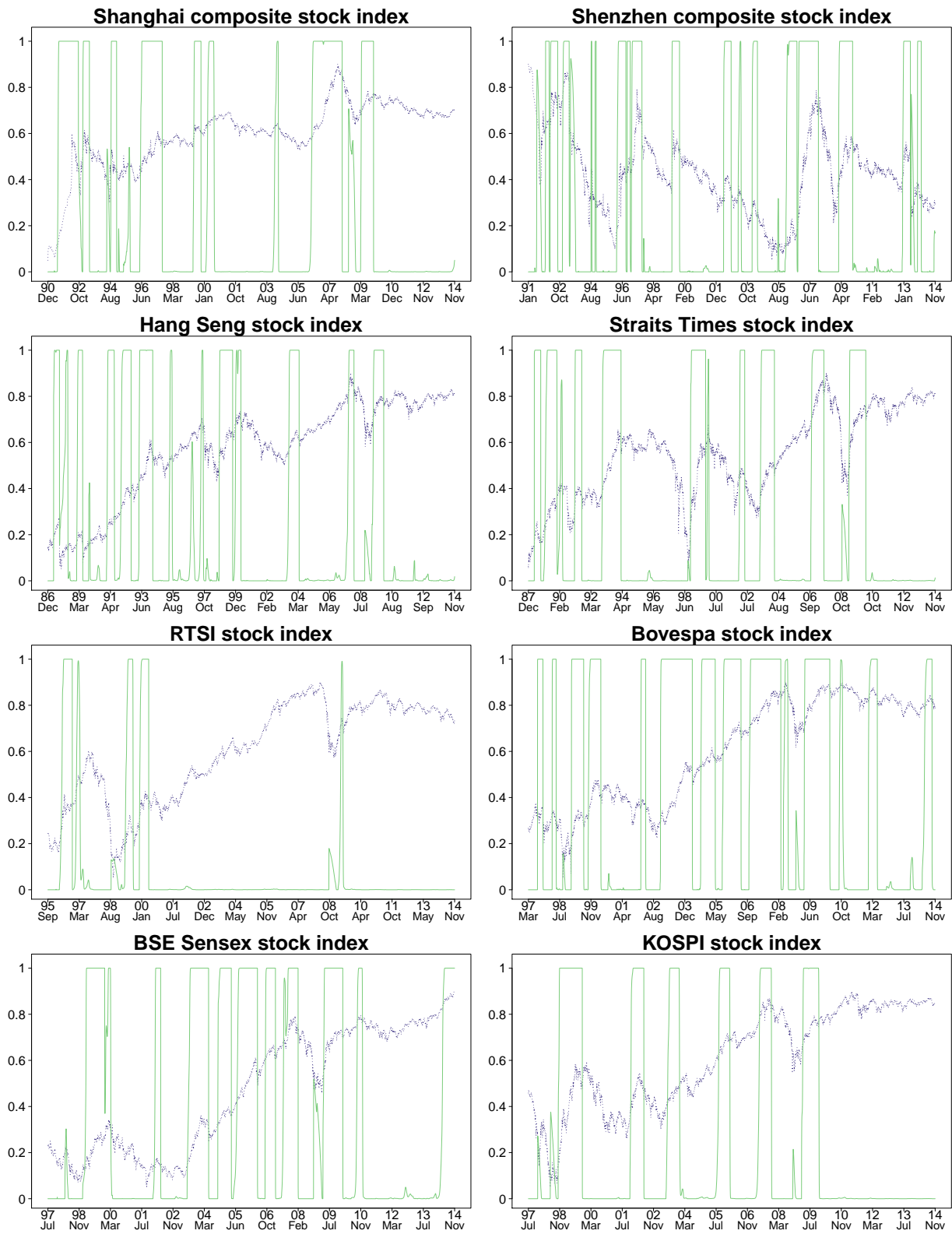


Figure 2: same as figure 1 for eight typical indices from stock exchanges of BRICs and other Asian markets, including China mainland, Hong Kong, Singapore, Russia, Brazil, India and Korea.

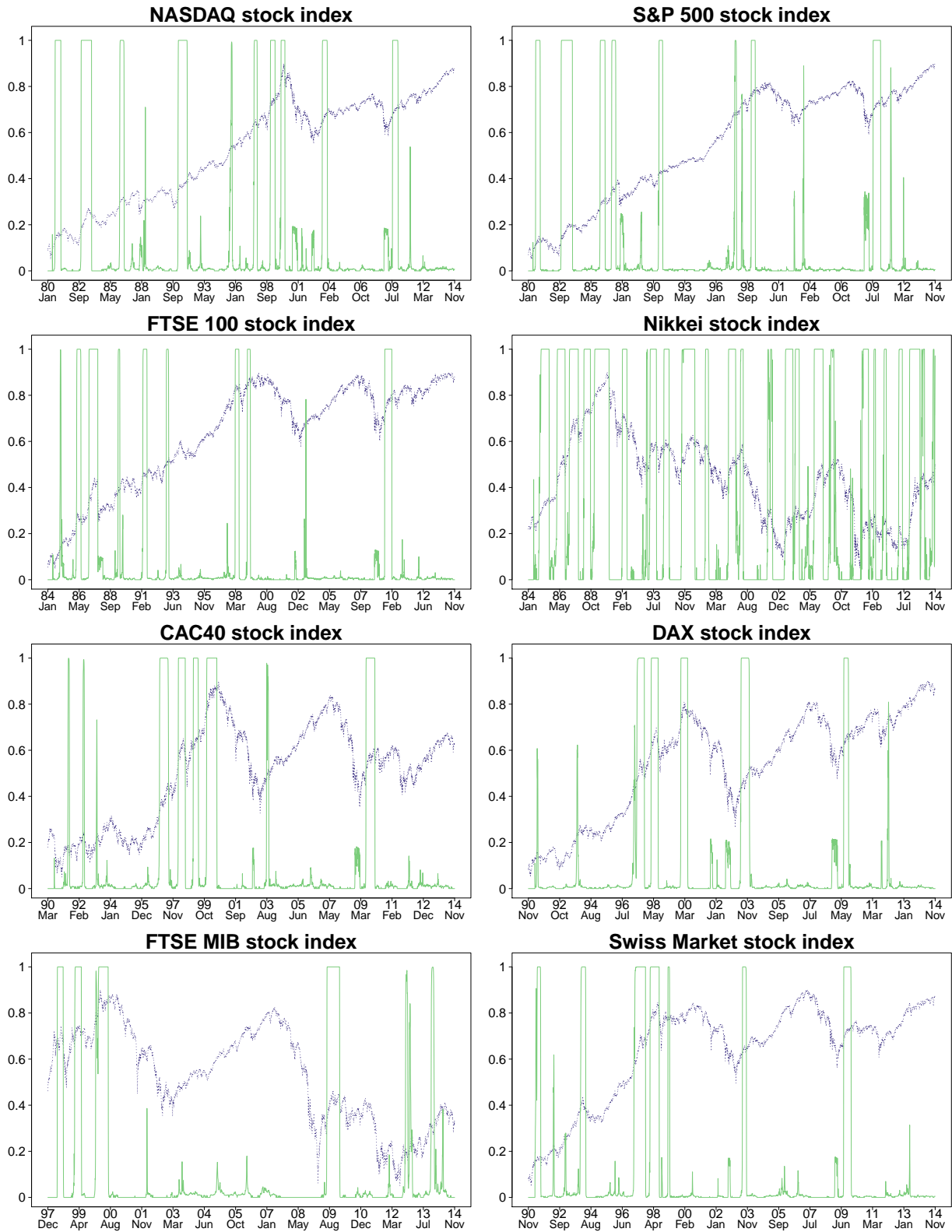


Figure 3: Estimated daily filtering probabilities $\langle s_t | y_{-\infty}^t \rangle$ of the periodical collapsing super-exponential growth bubble embedded in the Hidden Markov Modeling (HMM) procedure represented with the palegreen thin continuous curve bouncing between 0 and 1 for eight stock exchanges: U.S. (Nasdaq and S&P500), U.K., Japan, France, Germany, Italy and Switzerland. All indices are given in logarithmic scale and are rescaled into $[0,1]$ for comparison. In order to mitigate the effects of identifying regime-shift too often as a result of daily price volatility, all indices are geometrically averaged over 100 days according to $\ln p_t^{\text{filtered}} = (1/100) \sum_{i=0}^{99} \ln p_{t-i}$, before implementing the EM algorithm.

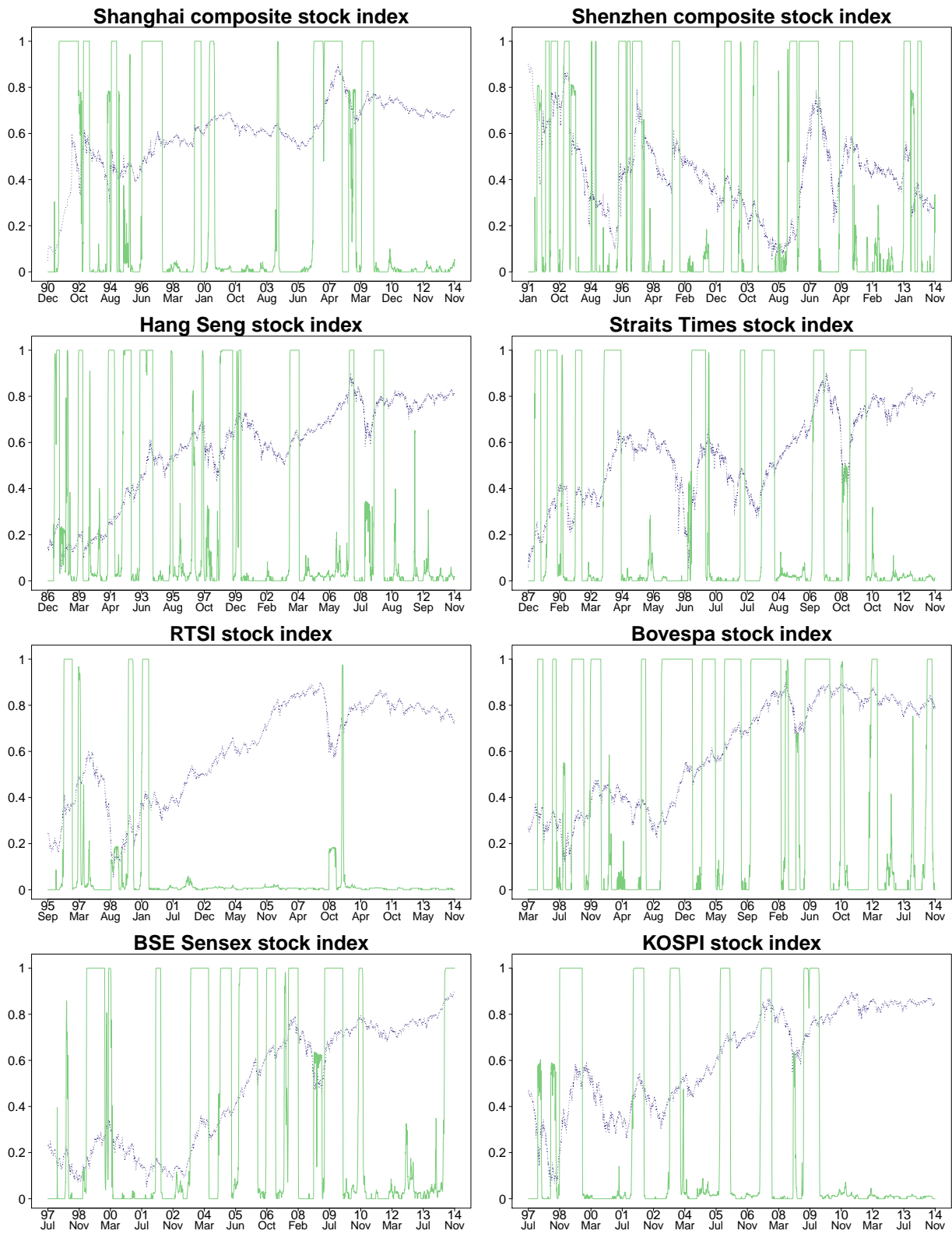


Figure 4: same as figure 3 for eight typical indices from stock exchanges of BRICs and other Asian markets, including China mainland, Hong Kong, Singapore, Russia, Brazil, India and Korea.

probability for the presence of super-explusive bubbles for the same sixteen global financial markets. The studied stock indices include the US NASDAQ index and S&P 500 stock index from the New York Stock Exchange, the FTSE 100 index from London Stock Exchange, the Nikkei 225 index from Tokyo Stock Exchange, the CAC40 stock index from Euronext Paris, the DAX index from Frankfurt Stock Exchange in Germany, Switzerland's blue-chip stock market index (SMI), the FTSE MIB stock index from Borsa Italiana, the two major stock indices from Chinese stock market (Shanghai composite index and Shenzhen composite index), the Hang Seng index from Hong Kong Stock Exchange, the Straits Times stock index from Singapore Exchange, the Russia Trading System (RTS) index from Moscow Stock Exchange, the Bovespa index from the São Paulo Stock, Mercantile & Futures Exchange, the SENSEX index from Bombay Stock Exchange in India and the Korea Composite Stock Price Index(KOSPI). In the implementation of our EM procedure, the condition of convergence of the algorithm is specified as

$$\Delta = \frac{\ln \mathcal{L}_{\theta^{(k+1)} | \theta^{(k)}} - \ln \mathcal{L}_{\theta^{(k)} | \theta^{(k-1)}}}{\ln \mathcal{L}'_{\theta^{(k)} | \theta^{(k-1)}}} \leq 0.0001 \quad (24)$$

Several observations are worth describing.

- There is an excellent correspondence between the estimated daily smoothing and filtering probabilities in essentially all cases: the periods identified in the super-exponential bubble state with the *smoothing probability* $\langle s_t | y_{\infty}^T \rangle$ using the information contained in the complete time series match remarkably closely those intervals identified in the super-exponential bubble state with the causal *filtering probability* $\langle s_t | y_{\infty}^t \rangle$ that use data up to the running present time t . This is perhaps not too surprising since our bubble detection method does not rely on the existence of a crash or change of regime but solely on the identification of a transient super-exponential dynamics.

- It is quite striking that the periods identified in the super-exponential bubble state are in general associated with a strong upward price dynamics (not a surprise from the construction of the model) ending with a peak of the price followed by a clear change of price regime (this second property being much less trivial). This change can take the form of a significant correction or crash, of a sideways volatile dynamics or of a downward price momentum. The presence of such changes of regime is a pleasant qualitative confirmation of one of the key insights of super-exponential models, namely the non-sustainable nature of the price dynamics that has to break into a slower growth, in fact often a reversal.

- While most bubble researchers would agree on the diagnostic of a bubble in a number of cases found to correspond to large values of our smoothing and filtering probabilities, such as during the price ascent associated with the dot-com bubble in Western markets, which is here correctly identified by our method, one could raise the criticism that many periods are picked out that do not correspond to the times of well-documented bubbles, raising the spectrum of too many false alarms (false positives or errors of type I). In response to this, we argue that, as said above, most of these identified bubble periods are followed by a significant change of price regime, which can be taken as a validation of the bubble identification. Moreover, it is the goal of a better model with superior implementation to indeed reveal hitherto hidden aspects of the price dynamics. Thus, it should not be a surprise that our method identifies a number of bubble regimes that would have not been suspected by other means. Figs. 1-4 thus lead us to conjecture that financial markets are much more often in bubble states than previously believed.

We have quantified the fractions of time, weighted by the corresponding probabilities, that the 16 studied markets are in a bubble. Table 1 below lists the results, with the fractions expressed as percentages. The notations p.b(filter) and p.b(smoothing) indicate the fractions of time when markets are in a bubble regime, as determined respectively by filtering probabilities and smoothing probabilities. These fractions are obtained as the integral of the corresponding probabilities shown in Fig. 1 - 4 over the whole time period for each of the 16 investigated markets. Except for the

Russian market with fractions as low as 8%, the chance for western stock markets to be in bubble regime is typically in the range 10%-15% cross-sectionally. In contrast, emerging markets as well as Japan market, the only developed market in Asia, are found about 20% to 45% of the time in the bubble regime. This may due to the less transparent information environment as well as weaker regulatory control, which tends to promote herding.

Table 1: Fractions of time that the sixteen studied stock markets are in bubble regime. We give the fractions with only two digits, as a higher precision would be provide a misleading sense of accuracy.

Stock Index	p.b(filter,%)	p.b(smoothing,%)
NASDAQ	15	16
SP500	12	12
FTSE	10	11
RTSI	8	9
CAC40	12	13
DAX	11	11
MIB	12	13
SMI	12	13
N225	40	43
SSEC	30	30
SZSC	32	32
HSI	24	25
STI	27	28
BVSP	46	46
SENSEX	36	38
KS11	23	23

- The previous remark raised the issue of false positives. What about false negatives or errors of type II? Some studies have suggested that the run-ups of stock market prices of Western markets from 2003 to 2007 qualify as a bubble (Sornette and Woodard, 2010; Sornette and Cauwels, 2014, 2015). In contrast, Figs. 1 and Fig. 3 give a zero bubble probability for this time interval for all Western markets. One likely explanation of these missed targets was advanced by Andersen and Sornette (2004), who stressed that, by construction the (Sornette and Andersen, 2002) model assumes that bubbles are associated to *both* a super-exponential price appreciation *and* a corresponding explosion of the volatility. But Andersen and Sornette (2004) showed that, for a number of historical bubbles, this is counterfactual: many bubbles develop without a clear increase of volatility, which would then lead the Sornette-Andersen model to be rejected. Indeed, many bubbles are developing over a time of complacent view of the underlying risks, in other words, the genuine risks are under-estimated and the crash often comes as a surprise. This led Andersen and Sornette (2004) to suggest the existence of at least two types of bubbles, the “fearful” (resp. “fearless”) bubbles associated with an increasing (resp. constant or decreasing) volatility. Our present investigation can thus be understood as targeting only the fearful bubbles.

3 Speculative Influence Network

3.1 Definitions

We introduce the *Speculative Influence Network* (SIN) as a directional weighted network of financial assets, such as stocks, bonds, mutual funds, real estate, forex, commodities, derivatives

and so on, which is organized to map the mutual relationships representing the speculative influences between them, i.e., how speculative trading of one asset may draw speculative trading in another assets. The arrow of a link in the SIN then indicates the direction of the speculative trading influence, and its weight quantifies the intensity of the influence. In order to derive the causal speculative influence between assets, we propose a two-steps procedure: (i) estimate for each asset the daily filtering probability for the presence of super-explosive bubbles using the HMM based approach developed in Section 2.2 with the regime-switching Sornette-Andersen bubble model; (ii) once two assets are diagnosed as being in a bubble state, identify the possible causal flow of the probabilities from one asset to the other in order to infer a possible influence or contagion effect. In other words, provided one asset X is diagnosed to be in a bubble, we want to estimate how much does it influences the probability of another asset Y to be also in the bubble state.

There are at least two well-known methods to detect causal relationship between time-series, the Granger Causality test and the information-based Transfer Entropy (TE) formulation. The former is relatively “cheaper”, being linear by construction, while the later encompasses nonlinear relationship and does not rely on a model specification. Although the Granger Causality test is more popular in economics and finance, it is mainly designed for multivariate linear autoregressive processes with white-noise residuals. For general nonlinear stochastic time series, it provides only an approximate measure of causal influence (Barrett and Barnett, 2013). Moreover, elegant proofs show that the two methods are only equivalent for Gaussian, exponential Weibman and log-normal variables (Barnett et al., 2009; Hlaváčková-Schindler, 2011). Our inputs are the time series of the *filtering probabilities* $\langle s_t | y_{-\infty}^t \rangle$ for all assets, which exhibit properties far from the conditions of application of the Granger Causality test: (i) the $\langle s_t | y_{-\infty}^t \rangle$'s are bounded in $[0, 1]$; (ii) they exhibit strong non-Gaussian characteristics with a pronounced bimodality near 0 or 1; there is no guarantee that they obey autoregressive processes. Therefore, we prefer to use the TE method in the remaining of the article.

3.2 Transfer Entropy

In his famous work “A Mathematical Theory of Communication”, Shannon pioneered a novel metric to quantify the uncertainty of an outcome from a set of possible events, the so-called Shannon Entropy. In order to capture the average uncertainty in a system that is comprised of a set of events with occurrence probabilities $p_i, i = 1, \dots, n$, the Shannon Entropy (SE) $H(p_1, p_2, \dots, p_n)$ is required to satisfy the following three properties:

1. $H(p_1, \dots, p_n)$ should be continuous in p_i .
2. If $p_i = \frac{1}{n}, i = 1, \dots, n$, then $H(p_1, \dots, p_n)$ should monotonically increase with n .
3. If an event i can be further broken down into several sub-events, then the SE is updated by adding the sums of the SE of such event with weights equal to their occurrence probabilities, i.e., $H_{\text{new}} = H_{\text{old}} + p_i H_i$, where H_i is the value of the function H for the composite event.

Then, it can be proved that these three properties lead to the unique Shannon Entropy function
$$H = - \sum_{i=1}^N p_i \log_s p_i = - \sum_{i=1}^N \langle i | \log_s \langle i |$$
 where the base s of the logarithm is arbitrary and depends on the chosen information units. For example, s is often selected to be equal to 2 when the measure is given in terms of bits of information. Shannon Entropy bears a lot of resemblance to Gibbs’ entropy, which quantifies the degree of diversity for a system’s possible micro-states. But SE is more general and gauges the necessary external information inflow needed to ascertain a specific micro-state for a event to happen.

When dealing with systems that interact with each other, the notion of *Transfer Entropy (TE)* can be introduced to describe the extent to which the uncertainty of one system is influenced

by other systems inter-temporally. Consider two systems U and V that are Markov processes of degree k_U and k_V respectively. Let us denote the sets of possible events for U and V at time t by u_t and v_t . Then, the TE from system V to U at time t is defined as

$$\begin{aligned}
TE_{V \rightarrow U}(t) &= - \sum_{\substack{u_t, \dots, u_{t-k_U} \\ v_{t-1}, \dots, v_{t-k_V}}} \langle u_t, \dots, u_{t-k_U}, v_{t-1}, \dots, v_{t-k_V} | \cdot \log_s \langle u_t | u_{t-1}, \dots, u_{t-k_U} \rangle \\
&\quad - \left(- \sum_{\substack{u_t, \dots, u_{t-k_U} \\ v_{t-1}, \dots, v_{t-k_V}}} \langle u_t, \dots, u_{t-k_U}, v_{t-1}, \dots, v_{t-k_V} | \cdot \log_s \langle u_t | u_{t-1}, \dots, u_{t-k_U}, v_{t-1}, \dots, v_{t-k_V} \rangle \right) \\
&= \sum_{\substack{u_t, \dots, u_{t-k_U} \\ v_{t-1}, \dots, v_{t-k_V}}} \langle u_t, \dots, u_{t-k_U}, v_{t-1}, \dots, v_{t-k_V} | \cdot \log_s \frac{\langle u_t | u_{t-1}, \dots, u_{t-k_U}, v_{t-1}, \dots, v_{t-k_V} \rangle}{\langle u_t | u_{t-1}, \dots, u_{t-k_U} \rangle}
\end{aligned} \tag{25}$$

According to the above definition, the TE from V to U is just the difference between the amount of uncertainty for U when merely measured based on its past information and its amount of uncertainty when also taking account of V 's past information. Hence, the TE effectively measures the reduction of uncertainty of system U achieved by using the information of system V . In other words, it provides an evaluation of the power of V to predict the motion of U . It quantifies the strength of the causal relationship between U and V . In the following subsection, we show how to use the TE to develop the SIN for financial markets.

3.3 Constructing the *Speculative Influence Network (SIN)* for a financial market

In the present work, the speculative influence relationship between two different financial assets is measured by calculating the TE between the time-series of the filtering probabilities defined in subsection 2.2 and illustrated in subsection 2.3, conditional on the two assets being in the bubble state. For this, we introduce the *speculative influence intensity (SII)* from X to Y as

$$SII_{X \rightarrow Y}(t) = TE_{p_b^f(X) \rightarrow p_b^f(Y)}(t), \tag{26}$$

where the time-series $p_b^f(X) = \{\langle s_t = 1 | \ln p_{X,t}, \ln p_{X,t-1}, \dots, \ln p_{X,0} \rangle\}_{t=0}^{t=T} = \{\langle s_t = 1 | x_{-\infty}^t \rangle\}_{t=0}^{t=T}$ and $p_b^f(Y) = \{\langle s_t = 1 | \ln p_{Y,t}, \ln p_{Y,t-1}, \dots, \ln p_{Y,0} \rangle\}_{t=0}^{t=T} = \{\langle s_t | y_{-\infty}^t \rangle\}_{t=0}^{t=T}$ respectively denote the estimated filtering probability of staying in the bubble state for assets X and Y .

According to the derivations presented in subsection 2.2, the filtering probability $\langle s_t | y_{-\infty}^t \rangle$ at time t only depends on the previous one $\langle s_{t-1} | y_{-\infty}^{t-1} \rangle$ at $t-1$ and on y_t . This is intended to capture the idea that the level of herding at a given time is mostly influenced by that of the previous time period (day in our empirical estimations). Using this property, formula (25) for the TE of V to U can be simplified into

$$\begin{aligned}
TE_{V \rightarrow U}(t) &= \sum_{u_t, u_{t-1}, v_{t-1}} \langle u_t, u_{t-1}, v_{t-1} | \cdot \log_s \frac{\langle u_t | u_{t-1}, v_{t-1} \rangle}{\langle u_t | u_{t-1} \rangle} \\
&= \sum_{u_t, u_{t-1}, v_{t-1}} \langle u_t, u_{t-1}, v_{t-1} | \cdot \log_s \frac{\langle u_t, u_{t-1}, v_{t-1} | \langle u_{t-1} |}{\langle u_t, u_{t-1} | \langle u_{t-1}, v_{t-1} |}
\end{aligned} \tag{27}$$

where U and V actually represent $p_b^f(X)$ and $p_b^f(Y)$, and correspondingly $u_t = \langle s_t = 1 | x_{-\infty}^t \rangle$ and $v_t = \langle s_t = 1 | y_{-\infty}^t \rangle$.

In order to use (27), we need to specify $\langle u_{t-1} |$, $\langle u_{t-1}, v_{t-1} |$, $\langle u_t, u_{t-1} |$ and $\langle u_t, u_{t-1}, v_{t-1} |$. For this, we divide the range $[0, 1]$ of $p_b^f(X)$ and $p_b^f(Y)$ in 10 bins of equal width and treat each bin as a unique identified event for gauging the presence of speculative herding. This coarse-graining procedure amounts to considering two events within a given bin as being undistinguishable and is performed to reduce the sensitivity to noise and minimize the impact of model mis-specification. Correspondingly, the base s in (27) is set to 10 for the practical computing. Then, by counting the number of different combinations associated with the value vector of time-series U up to a certain day, with the vector for U 's values lagged by one day and with the vector for V 's values also lagged by one day, all four distributions $\langle u_{t-1} |$, $\langle u_{t-1}, v_{t-1} |$, $\langle u_t, u_{t-1} |$ and $\langle u_t, u_{t-1}, v_{t-1} |$ can be empirically calculated. $\langle u_{t-1} |$ is obtained by taking the ratio of the number of times a $\langle u_{t-1} |$ in a given bin appeared in the vector U by the total number of occurrences for all bins types. In order to estimate $\langle u_{t-1}, v_{t-1} |$, one must count how many times a particular combination of bins, that the couple states (u, v) belongs to, appeared in the joint vector of lagged U 's values and lagged V 's values, and then normalise by the total number of occurrences for the pairs. The calculation of $\langle u_t, u_{t-1}, v_{t-1} |$ is similar to that of $\langle u_{t-1}, v_{t-1} |$, except that the counting is conducted on bins triplets that appear in the vector obtained by joining all three vectors. The calculation of SII between arbitrary pairs of two investment targets finally gives the SII matrix for the whole financial market, which is the basic encoding scheme to derive the adjacency matrix that defines the SIN.

The assets of interest are the nodes of the SIN. A relationship in which node X_i influences node X_j is quantified by $\text{SII}_{X_i \rightarrow X_j}$ and is represented by a directed link $X_i \rightarrow X_j$. This does not exclude the possible existence of a direct influence in the opposite direction from node X_j to node X_i measured by $\text{SII}_{X_j \rightarrow X_i}$, making the SIN a bilateral directional network. In practice, we use a threshold so that values of $\text{SII}_{X_i \rightarrow X_j}$ below this threshold are considered too small to be of significance and only the transfer entropies larger than this threshold will be used in the SIN representation. To further extract the leading influence relationship, we introduce the *net speculative influence intensity* (NSII)

$$\text{NSII}_{X_i \rightarrow X_j}(t) = \text{SII}_{X_i \rightarrow X_j}(t) - \text{SII}_{X_j \rightarrow X_i}(t), \quad (28)$$

allowing us to reduce SIN to an unidirectional network capturing the net influence effects between assets. In this reduced unidirectional SIN, only positive NSII values need to be considered and are represented as arrows going from the influencer i to the receiver j (for $\text{NSII}_{X_i \rightarrow X_j}(t) > 0$).

4 Early warnings of bubbles for Chinese Markets via SIN

4.1 Data and methodology

We now investigate empirically how the Speculative Influence Network (SIN) can help provide effective early warning signals by dissecting a bubble structure via a disaggregated firm level analysis. We show below that the SIN complements the more conventional bubble detection method based on super-exponential growth signatures of the aggregated market, by providing indicators of strong speculative influence (or contagion) that can be useful by playing the role of systemic risk gauges. Our tests consist in quantifying the out-of-sample performance of the prediction of the maximum cumulative lost proportion (%MaxLoss) of each asset based on the SIN analysis.

We focus our attention on the Chinese stock market and on the special periods from 2006 to 2008 when the stock market exhibited remarkable signatures of speculation and bubble behavior. Jiang et al. (2010) have provided a detailed synthesis of this episode, using the log-periodic power law singularity model. Following a bearish trend that lasted nearly 5 years, the Chinese

stock market rebounded in 2005. The most representative stock index for the market of A-shares, the Shanghai Stock Exchange Composite index (SSEC), reached its lowest point in 2005 at the level 998. It rose exuberantly up to 6124 (corresponding to a relative appreciation of 513.5%) over a mere two years interval. Meanwhile, the second most important index, the Shenzhen Stock Exchange Component index (SZSC), reached a peak of 19600 from its historical lowest point at 3372 (corresponding to a relative appreciation of 481.2%) over just eighteen months. Correspondingly, the total market value for all stocks traded both in the Shanghai Stock Exchange (SHSE) and in the Shenzhen Stock Exchange (SZSE) has grown explosively from 30 trillion yuan at the beginning of 2005 to about 250 trillion yuan at the peak in October 2007. This made China's stock market temporarily the World's third largest market. Since its peak in 17th October 2007 at 6124, the SSEC has dropped to the low of 1664 on 28th October 2008. Similarly, after its peak at 19600 on the 10th of October 2007, the SZSC reached its bottom at 5577.33 on the 28th of October 2008. For both markets, the total drawdown from peak-to-valley corresponds to a loss in excess of 70% in just one year, surpassing all the losses incurred during the bearish period from 2001 to 2005. Such impressive and breathtaking roller-coaster performance with extraordinary quintupling of the value of the main Chinese financial indices in less than two years accompanied by a rapid shrinkage in just one year back to a longer trend make the Chinese stock market an ideal specimen on which to test our proposed analytics.

For the purpose of constructing the early warning signals, the SIN of the Chinese stock market is constructed within the window from 2006 to the end of 2007, covering the period when the market is still in its growth regime, without significant large financial sell-offs. The assets we consider to construct the SIN are the Sector Series from the CSI 300 index, which are compiled by the China Securities Index Company, calculated since April 8, 2005 and designed to replicate the performance of 300 stocks traded either in SHSE or in SZSE with outstanding liquidity and size. The sector series are sub-indices based on the stocks in the CSI 300 that reflect specific industrial sectors. There are ten CSI 300 sector indices in total: Energy, Materials, Financial, Industrials, Consumer Discretionary, Consumer Staples, Health Care, Information Technology, Telecommunications and Utilities. Because of the special role played by the financial sector in terms of its almost unique large leverage, its essential role as credit provider to the economy, and given its recognized responsibility in propagating systemic shocks to other sectors of the economy, we disaggregate the CSI 300 Financial Index into its individual firm components, according to the classification by China Securities Regulatory Commission.

Table 2 lists some basic descriptive statistics for the nine industrial indices covered in this article. In the putative bubble phase starting from 2006 to the end of 2007, the table gives the maximum and minimum values of those indices as well as their daily return μ and volatility σ (estimated based on a specification in terms of a geometric Brownian motion and shown in percentage form). The sixth and seventh columns respectively show the fraction of filtering probabilities calculated daily (based on the method presented in subsections 2.2 and 2.3) that meet particular criteria over the period. Specifically, column h.f.p(%) gives the percentage of times when the filtering probability is larger than 0.9. Column l.f.p(%) gives the percentage of times when the filtering probability is smaller than 0.1, indicating that the speculative bubble behavior is fading away on that sector while it is active for the overall market. The last column (%MaxLoss) gives the maximum percentage loss for each industrial sector over 2008. This loss is defined as the RMB amount of the maximum cumulative decline in market capitalization of the corresponding representative stock index during 2008 divided by the maximum market capitalization in 2008. Similarly, Table 3 lists the same basic descriptive statistics for the financial firms constituting the Financial CSI 300 sector index. There are 22 financial stocks respectively belonging to four sub-sectors: bank, securities, trust and insurance. Comparing the two tables, it is quite impressive to note the much larger variations of these basic statistics at the disaggregated financial firm level in Table 3 compared to the non-financial sectors level in Table 2. One can also observe that the

stocks of securities or trust companies exhibit larger daily volatility than bank and insurance companies. However, such facts have little relation with the observed proportion of speculative days h.f.p(%) and with %MaxLoss.

Table 2: Descriptive statistics for the nine chosen representative Chinese industrial indices. Column h.f.p(%) gives the percentage of times when the filtering probability is larger than 0.9. Column l.f.p(%) gives the percentage of times when the filtering probability is smaller than 0.1. The last column (%MaxLoss) gives the maximum percentage loss for each industrial sector over 2008 as defined in the text.

Industrial Sectors	time window: 2006-2007						2008
	Min	Max	$\mu(\%)$	$\sigma(\%)$	h.f.p.(%)	l.f.p.(%)	%MaxLoss
Energy	1078.1	7740.5	0.37	2.32	40.90	48.47	73.75
Materials	868.3	6419.4	0.38	2.23	27.64	59.23	76.03
Industrials	884.0	5342.9	0.36	2.04	26.60	61.34	73.35
Consumer Discretionary	893.4	5332.9	0.35	2.19	29.62	59.10	71.95
Consumer Staples	1052.1	7501.9	0.41	2.06	28.71	59.66	65.91
Health Care	833.7	5242.2	0.37	2.28	28.07	62.38	59.65
Information Technology	727.5	2694.1	0.26	2.27	28.80	54.46	74.31
Telecommunications	950.6	4163.0	0.29	2.36	20.54	72.39	67.29
Utilities	879.5	3738.9	0.28	2.19	30.31	60.01	60.07

In order to exploit the SIN analysis, we define a set of indicators that measure the speculative influence effects at diverse levels of aggregation. The set made of the nine industrial sector nodes is denoted by \mathcal{G}_I . The set made of the 22 financial institution nodes is denoted by \mathcal{G}_F .

1. *SI-to-All* measures the total speculative influence of a given node i to all other nodes, including the industrial sectors and financial institutions:

$$SI\text{-to-All}_i = \sum_{\substack{j \in \mathcal{G}_I \cup \mathcal{G}_F \\ j \neq i}} SII_{i \rightarrow j} . \quad (29)$$

This indicator will allow us to identify those nodes that have a significant global influence on the entire network.

2. *SI-from-All* measures the total speculative influence of all other nodes including industrial sectors and financial institutions on a given node i :

$$SI\text{-from-All}_i = \sum_{\substack{j \in \mathcal{G}_I \cup \mathcal{G}_F \\ j \neq i}} SII_{j \rightarrow i} . \quad (30)$$

This indicator identifies the sectors or firms that are the most susceptible to the overall speculative influence of the network.

3. *SI-to-Fin* measures the total speculative influence of a given node i to all financial institution nodes:

$$SI\text{-to-Fin}_i = \sum_{\substack{j \in \mathcal{G}_F \\ j \neq i}} SII_{i \rightarrow j} . \quad (31)$$

This indicator quantifies how certain institution and sector's speculative behavior may influence the financial sector firms.

Table 3: Descriptive statistics for 22 chosen stock prices belonging to the financial sector. Same definitions as Table 2.

Financial Institution	Abbr.	Sub-sectors	window: 2006-2007						2008
			Min	Max	$\mu(\%)$	$\sigma(\%)$	h.f.p.(%)	l.f.p.(%)	%MaxLoss
Ping An Bank	PAB	Bank	165.9	1440.2	0.44	3.26	27.10	67.32	75.43
Hong Yuan Securities	HYS	Securities	12.0	202.2	0.59	4.25	20.75	71.48	76.23
Shaanxi International Trust	SIT	Trust	11.4	111.8	0.45	4.21	11.81	82.38	73.51
Northeast Securities	NES	Securities	9.0	369.2	1.26	12.38	8.75	85.41	81.61
Guoyuan Securities Company	GSC	Securities	2.9	61.8	1.26	10.30	11.42	81.66	78.27
Changjiang Securities Company	CJSC	Securities	4.9	76.9	1.18	10.63	30.15	60.79	77.17
Shanghai Pudong Development Bank	SPDB	Bank	16.0	125.1	0.44	3.20	34.75	55.88	76.66
Hua Xia Bank	HXB	Bank	6.2	40.2	0.40	3.34	23.39	67.71	71.06
China Minsheng Banking Corp.	CMBC	Bank	19.3	146.2	0.37	2.89	26.38	64.19	68.69
Citic Securities Company	CSC	Securities	7.2	162.9	0.62	3.79	14.87	80.84	66.84
China Merchants Bank	CMB	Bank	13.4	110.0	0.43	2.78	28.63	60.66	73.86
Sinolink Securities	SLS	Securities	4.5	166.7	0.88	5.92	13.68	82.47	69.85
Southwest Securities	SWS	Securities	2.1	18.3	0.96	3.20	24.15	71.95	78.45
Anxin Trust	AXT	Trust	12.9	152.2	0.78	4.75	11.52	84.59	72.66
Haitong Securities Company	HSC	Securities	38.0	626.8	0.61	4.33	6.99	89.92	75.51
Industrial Bank	CIB	Bank	22.2	67.7	0.40	3.24	26.78	66.20	80.68
Ping An Insurance (Group)	PAIC	Insurance	44.4	145.7	0.40	3.04	38.04	54.41	80.77
Bank Of Communications	CCB	Bank	10.4	16.8	0.09	2.78	21.62	72.99	73.09
Industrial And Commercial Bank	ICBC	Insurance	3.3	8.9	0.32	2.74	22.88	71.18	57.76
China Life Insurance Company	CLIC	Insurance	32.0	75.3	0.17	3.24	29.33	61.64	68.72
Bank Of China	BOC	Bank	3.2	7.5	0.15	2.41	24.59	65.31	56.69
China Citic Bank Corp.	CITIC	Bank	8.5	12.6	-0.07	2.97	30.83	59.90	64.21

4. *SI-from-Fin* measures the total speculative influence of all financial nodes onto a given node i :

$$\text{SI-from-Fin}_i = \sum_{\substack{j \in \mathcal{G}_F \\ j \neq i}} \text{SII}_{j \rightarrow i}. \quad (32)$$

5. *SI-to-IX* measures the total speculative influence of a given node i to all other nodes of the industrial sectors (excluding the financial institutions):

$$\text{SI-to-IX}_i = \sum_{\substack{j \in \mathcal{G}_I \\ j \neq i}} \text{SII}_{i \rightarrow j}. \quad (33)$$

6. *SI-from-IX* measures the total speculative influence of all other nodes of the industrial sectors (excluding the financial sector) on a given node i :

$$\text{SI-from-IX}_i = \sum_{\substack{j \in \mathcal{G}_I \\ j \neq i}} \text{SII}_{j \rightarrow i}. \quad (34)$$

In addition, using the *net speculative influence intensity* (NSII) defined by (28) leading to a unidirectional network, we shall also use the following indicators obtained from (29-34) as

follows:

$$\text{NSII-on-All}_i = \sum_{\substack{j \in \mathcal{G}_I \cup \mathcal{G}_F \\ j \neq i}} \text{NSII}_{i \rightarrow j} = \text{SI-to-All}_i - \text{SI-from-All}_i \quad (35)$$

$$\text{NSII-on-Fin}_i = \sum_{\substack{j \in \mathcal{G}_F \\ j \neq i}} \text{NSII}_{i \rightarrow j} = \text{SI-to-Fin}_i - \text{SI-from-Fin}_i \quad (36)$$

$$\text{NSII-on-IX}_i = \sum_{\substack{j \in \mathcal{G}_I \\ j \neq i}} \text{NSII}_{i \rightarrow j} = \text{SI-to-IX}_i - \text{SI-from-IX}_i . \quad (37)$$

These indicators quantify the net speculative influence flux of a node to all the other nodes (NSII-on-All_i), to all financial nodes (NSII-on-Fin_i) and to all non-financial nodes (NSII-on-IX_i).

We want to detect what combination of indicators for individual institution/sector performs best as the leading factor during a bubble phase to explain the %MaxLoss of a given node associated with a large financial sell-offs during a bubble collapse. The corresponding leading factors are good candidates to provide early-warning signals encoded in the SIN and to become systemic risk metrics.

4.2 Early-warning signal extraction from the speculative influence network (SIN)

To evaluate the predictive power of SIN indicators defined above, we first perform multivariate regressions of %MaxLoss on different combinations of the 6 indicators (29-34). For the purpose of completeness and to avoid unnecessary multicollinearity, 17 regression models in total are selected. On the basis that industrial sectors and financial institutions play different roles, we simplify the treatment by performing tests on group \mathcal{G}_F and group \mathcal{G}_I separately. The results are shown in tables 4 and 5. All indicators are constructed with data from 1st January 2006 to 31st December 2007 and they are ranked before implementing the regressions. Without loss of information and to avoid inflating the tables, we do not report the intercepts of the regressions.

For Chinese financial institutions, we find that SI-to-Fin and SI-from-Fin are both significant determinants to explain their maximum drawdown in 2008, while their impacts are of opposite signs. The positive sign obtained for the ranked value of SI-to-Fin means that the more powerful is the speculative herding influence of a node towards a financial institution, the larger is the loss of that node during the bubble burst. These results suggest the institutions with higher SI-to-Fin rank are more likely to act as the leading speculative engines of the overall speculative mania within the financial sector, with more inflow of speculative money during bubble. The negative sign obtained for the ranked value of SI-from-Fin implies that the larger is the speculative influence of financial institutions towards a given node, the stronger is the resilience of that node during the financial sell-offs. The institutions with higher SI-from-Fin rank are more likely to be lagging in the speculative frenzy and may be less exposed to the bubble collapse.

Table 4 demonstrates that SI-to-IX has also a high explanatory power for the loss sizes of industrial institutions (excluding financial firms). However, different from SI-to-Fin, the larger the speculative influence of a node on other industrial sector firms, the smaller is the loss during the crash. In contrast, SI-from-IX has an insignificant effect, suggesting that there is little transmission of speculation from the industry sectors to other firms. Additionally, table 4 also shows that SI-to-IX has a high explanatory power for the loss sizes of financial institutions. Again, different from SI-to-Fin, the larger the speculative influence of a node on all nodes of the industrial sectors, the smaller is the loss during the crash for this financial institution. We also observe that the risk transfer between financial institutions and industrial sectors is not symmetric. Table 5 shows that

there is little influence of the variable SI-to-Fin onto the industrial sector concerning its loss size. Meanwhile, given the insignificance of the variable SI-from-IX to explain the losses of financial institutions shown in table 4, we conjecture that, during the bubble, the Chinese financial sector as a whole only provided speculative money to other industrial sectors but did not absorb it back during the crisis.

As shown in table 5, SI-to-IX and SI-from-IX both become significant determinants of the losses of the industrial sector in 2008. This is very similar to the results obtained for financial institutions listed in table 4. This also suggests that the nodes that have the leading speculative influence on their peers bear the largest loss risks, while the followers are less punished by the market correction. However, we failed to find SI-from-Fin to be a significant indicator for %MaxLoss of industrial sectors. At first glance, this appears to be in contradiction with our previous conjecture that speculative money is more likely to go to industrial sectors, and taken out of financial institutions that have more influence onto industrial sectors as a whole. Noting that the financial sector as a whole is nothing but a peer node within the network of all industrial sectors, it is possible that the total flow of speculative money emanating from the financial sector is not sufficient to increase the risk exposure of the industrial sectors for this Chinese bubble. The %MaxLoss of industrial sectors should be in large part explained by the overall circulation of speculative money among all the nodes within the network rather than by the flow to and from a single node, such as the financial sector. In other words, this shows the limit of a simple causal analysis of influences, suggesting the importance of a complex nonlinear set of mutual interactions that cannot be simply linearly disentangled. In hindsight, this interpretation is also partially supported by the lack of evidence of the presence of systemic risks spreading from the financial sector to other Chinese economic sectors through illiquidity, insolvency, or losses during the bubble collapse.

We also performed correlation tests between %MaxLoss and possible combinations of our chosen indicators. To keep in line with the previously revealed relationships, the test first focuses on NSII and then associates NSII with a possible global influence effect for specific sub-networks, without making an exhaustive enumeration of all possible combinations. Similar to the above regression analysis, the tests are implemented separately on group \mathcal{G}_F and group \mathcal{G}_I . All combinations are ranked before testing. Table 6 presents the results based on three popular correlation statistics. We find that NSII-on-IX outperforms other combinations to predict the rank of loss sizes of industrial sectors. By taking account of other overall influence effects, the predictive power decreases in agreement with our previous discussion of the regression analysis that the financial sector had very little influence in transferring risks to other industrial sectors during this bubble. Nevertheless, NSII-on-Fin has only a modest correlation with the %MaxLoss for financial institutions. However, when considering SI-from-IX, its predictive power increases nearly twofold to become a significant signal. In agreement with our previous inference that financial institutions do not show significant tendencies to draw “hot money” from the real economy sector but act more as speculative followers, the present correlation estimations confirm that financial institutions are less important in China with respect to the systemic risks building up during the bubble, which is driven more by the real economy than the reverse.

To fully appreciate the impact of the relationships of speculation influence among various industrial sectors as well as financial institutions, Fig. 5 provides a visualization of the unidirectional SIN calculated by using data in the same time window as before (1st Jan. 2006 to 31 Dec. 2007). This network is comprised of two sub-networks, the industrial sectors with 9 nodes and the financial sub-network with 22 nodes. Recall that this financial network can be regarded as a special node in the former network but has been disaggregated as explained above.

First, the size of a node encodes the *net* transfer entropy (TE) from that node to all other nodes. To make the network representation comparable with the regression and correlation analyses presented above, we use a slightly different rule for the sizes of the nodes corresponding to the industrial sectors and to the financial firms. For the industrial sector nodes, their sizes are

Table 4: Test of the explanatory power of combinations of indicators described in the text from 1st Jan. 2006 to 31st Dec. 2007 to predict its Max% Loss over 2008 of the set of 22 financial institution nodes \mathcal{G}_F , with a multiple regression analysis. There are six candidate explanatory variables to be chosen: SI-from-All, SI-to-Fin, SI-from-Fin, SI-to-IX, SI-from-IX. In practice, these explanatory variables are transformed into their cross-sectionally ranked value before the regressions.

	Model1	Model2	Model3	Model4	Model5	Model6	Model7	Model8	Model9	Model10	Model11	Model12	Model13	Model14	Model15	Model16	Model17
SI-to-All	-0.25 (0.23)																
SI-from-All		-0.29 (0.22)															
SI-to-Fin			-0.18 (0.23)				0.03 (0.22)	0.17 (0.55)	-0.11 (0.22)				1.06* (0.52)	0.02 (0.23)	0.25 (0.53)		1.17* (0.58)
SI-from-Fin				-0.23 (0.23)				-0.38 (0.55)		-0.13 (0.21)		-0.17 (0.22)	-1.05** (0.49)		-0.39 (0.53)	-0.13 (0.21)	-1.15** (0.54)
SI-to-IX				-0.53** (0.20)			-0.54** (0.22)			-0.50** (0.21)	-0.48* (0.27)		-0.74*** (0.23)	-0.49 (0.30)	-0.46 (0.28)	-0.86** (0.32)	
SI-from-IX					-0.39 (0.22)				-0.37 (0.22)		-0.07 (0.27)	-0.36 (0.22)		-0.07 (0.28)	-0.37 (0.23)	-0.07 (0.28)	0.14 (0.28)
R ²	0.06	0.08	0.03	0.26	0.05	0.14	0.26	0.05	0.15	0.27	0.26	0.17	0.41	0.26	0.18	0.27	0.42
Adj. R ²	0.01	0.03	-0.02	0.22	-0.00	0.10	0.18	-0.05	0.06	0.20	0.18	0.08	0.31	0.14	0.04	0.15	0.28
F statistic	1.24	1.64	0.58	6.90	0.99	3.24	3.29	0.52	1.68	3.56	3.33	1.88	4.11	2.11	1.27	2.27	3.02

*** $p < 0.01$, ** $p < 0.05$, * $p < 0.1$

Table 5: Test of the explanatory power of combinations of indicators described in the text from 1st Jan. 2006 to 31st Dec. 2007 to predict its Max% Loss over 2008 of the set of nine industrial sector nodes \mathcal{G}_I , with a multiple regression analysis. There are six candidate explanatory variables to be chosen: SI-from-All, SI-to-IX, SI-from-IX, SI-to-Fin, SI-from-Fin. In practice, these explanatory variables are transformed into their cross-sectionally ranked value before the regressions.

	Model1	Model2	Model3	Model4	Model5	Model6	Model7	Model8	Model9	Model10	Model11	Model12	Model13	Model14	Model15	Model16	Model17
SI-to-All	0.64 (0.82)																
SI-from-All		0.57 (0.83)															
SI-to-IX				1.09 (0.75)			1.11 (0.78)			1.05 (0.81)	2.48** (0.91)		1.20 (0.89)	2.48** (0.94)		2.43* (0.98)	2.55* (1.06)
SI-from-IX					-0.07 (0.86)				-0.05 (0.90)		-1.89* (0.91)	-0.12 (0.91)		-1.86 (0.94)	-0.08 (1.02)	-1.88 (0.98)	-1.85 (1.04)
SI-to-Fin			0.49 (0.84)				0.53 (0.78)	0.33 (1.63)	0.49 (0.90)				0.96 (1.60)	0.48 (0.64)	0.30 (1.84)		0.84 (1.34)
SI-from-Fin					0.46 (0.84)			0.19 (1.63)		0.31 (0.81)		0.48 (0.91)	-0.51 (1.62)		0.22 (1.85)	0.29 (0.67)	-0.43 (1.35)
R ²	0.08	0.06	0.05	0.23	0.04	0.00	0.29	0.05	0.05	0.25	0.56	0.04	0.30	0.60	0.05	0.57	0.61
Adj. R ²	-0.05	-0.07	-0.09	0.12	-0.09	-0.14	0.05	-0.27	-0.27	0.00	0.41	-0.27	-0.12	0.36	-0.52	0.31	0.22
F statistic	0.62	0.48	0.34	2.13	0.31	0.01	1.21	0.15	0.15	1.01	3.75	0.14	0.72	2.50	0.09	2.22	1.57

*** $p < 0.01$, ** $p < 0.05$, * $p < 0.1$

Table 6: Correlations between %MaxLoss and different combinations of indicators given in the first column, as described in the text.

Indicators	Correlation Statistics		
	Pearson	Spearman	Kendall
For Industrial Sectors			
NSII-on-All	-0.06	-0.07	-0.06
NSII-on-IX	0.41	0.42	0.28
NSII-on-Fin	-0.25	-0.28	-0.22
NSII-on-IX-(SI-from-Fin)	-0.14	-0.10	-0.06
NSII-on-Fin-(SI-from-IX)	-0.37	-0.32	-0.22
NSII-on-IX+(SI-to-Fin)	0.22	0.27	0.17
NSII-on-Fin+(SI-to-IX)	0.12	0.10	0.06
For Financial Institutions			
NSII-on-All	0.29	0.20	0.13
NSII-on-Fin	0.28	0.22	0.15
NSII-on-IX	0.00	-0.06	-0.06
NSII-on-Fin-(SI-from-IX)	0.47	0.39	0.30
NSII-on-IX-(SI-from-Fin)	0.21	0.06	0.06
NSII-on-Fin+(SI-to-IX)	0.03	-0.02	-0.01
NSII-on-IX+(SI-to-Fin)	-0.22	-0.15	-0.14

determined by the rank value of their NSII-on-IX. For the financial institution nodes, their sizes are proportional to the ranked value of their NSII-on-Fin minus SI-from-IX.

In Fig. 5, all nodes are connected by their speculative influence relationship according to the NSII indicator defined by expression (28), i.e., an arrow from node X to Y indicates that X has a net positive influence to foster speculative trading on Y . The thickness of each arrow encodes the magnitude of the total of 465 NSIIs between 32 nodes. In details, the NSIIs are rescaled into $[0, 1]$ by a dilation transformation. Then, the thicknesses of the edges in the SIN are proportional to the rescaled NSIIs. To avoid overloading the figure, only the links with NSIIs that are above a threshold are represented with an arrow, as they represent the most important speculative influence relationships. In practice, the threshold was chosen to be $NSII \geq 0.3$, which yields 58 instances that account for approximately 10% of all links.

Finally, the color of a node encodes the rank of its %MaxLoss as shown on the scale in the figure inset. The two different kinds of nodes (industry and finance) are considered separately when calibrating the mapping function for node size and color.

Based on the colors and sizes of the nodes, the main information that emerges from Fig. 5 is that the sectors or firms that lost the most are those influencing others most. The second message of Fig. 5 is conveyed by the directions and thicknesses of the arrows. One can observe that some of the large nodes (e. g. Materials, Energy, CCB) receive many arrows pointing to them. Given that their sizes encode the fact that they are the largest net influencers, the arrows pointing to them reveals a second order effect that they also receive large influences (above the threshold $NSII \geq 0.3$) from a few other sectors or firms. But these large influences only contribute a maximum of 10% of the total influence relationships. Thus, it is more the overall influence over most of the other sectors and firms that dominate the amplitude of the losses, rather than the (large) influence of a few. Rather than identifying a few systemically important sectors, the SIN analysis

emphasises the role of aggregated speculative influences in determining global interconnectedness and systemic risks. This interpretation is consistent with the results of the above regression and correlation analyses, which have concluded that larger Net Transfer Entropies lead to larger losses.

The case of CITIC is special, as it seems to act as a hub for important two-way speculative influences between financial and industrial sub-networks. With smaller NSII-on-Fin minus SI-from-IX effect, this financial institution is, as expected, mildly punished during market correction. At first glance, The Information Technology sector seems to be an exception with little net entropy transfer to and from other industrial sectors but nevertheless a relative large loss. This can however be rationalized by the important influence relationship from the financial sector (in particular CITIC) that might also signal an invisible “hot money” transfer between the sector before the full force of speculative herding revealed itself.

5 Conclusion

We have introduced the Speculative Influence Network (SIN) to represent the causal relationships between sectors (and/or firms) during financial bubbles. The construction of SIN required two steps. First, we have shown how to estimate in real time the probability of speculative trading in each stock in the basket of interest, using a bubble identifying technique based on the Sornette-Andersen (2002) stochastic bubble model. We have augmented the Sornette-Andersen (2002) model by using a Hidden Markov Model (HMM), which was specially designed to calibrate regime-switching between normal and bubble regimes. Conditional on two stocks or two sectors being qualified in a bubble regime, we have introduced the *Transfer Entropy*, which quantifies the casual relationship between them. The transfer entropy provided a natural way to construct an adjacency matrix and thus to introduce the SIN. We have applied this methodology to the Chinese stock market during the period 2005-2008, during which a normal phase was followed by a spectacular bubble ending in a massive correction. Introducing the Net Speculative Influence Intensity (NSII) variable as the difference between the transfer entropies from i to j and from j to i , we have demonstrated its skill to predict the maximum loss (%MaxLoss) endured during the crash by the sectors and stocks. The statistically significant regressions and the graphical network representation has allowed us to illustrate the matrix of influences among sectors during the Chinese bubble. One the most striking result is the importance of the industrial sectors in influencing the financial firms and not vice-versa, showing a very different interaction structure than in western markets. We have also shown that the bubble state variable calibrated on the Chinese market data corresponds well to the regimes when the market exhibits a strong price acceleration followed by clear change of price regimes.

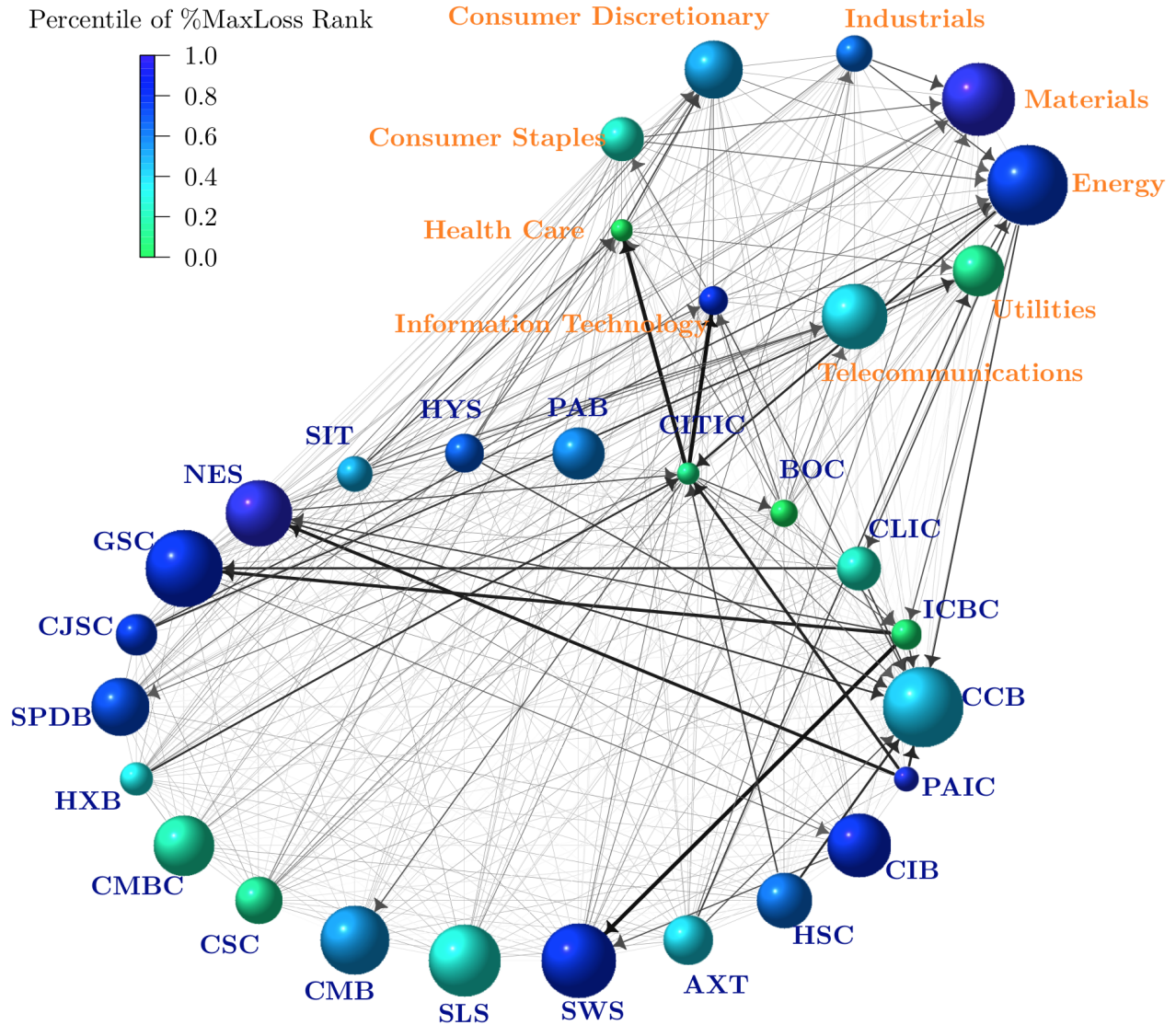


Figure 5: The unidirectional Speculative Influence Network (SIN) for the Chinese stock market constructed for the time interval from 1st Jan. 2006 to 31st Dec. 2007. This network is comprised of two sub-networks, the industrial sectors with 9 nodes and the financial sub-network with 22 nodes. The arrows connecting nodes represent the speculative influence relationship according to the NSII indicator defined by expression (28). The size of a node is determined by its net transfer entropy (TE) from that node to all other nodes. The color of a node encodes the rank of its %MaxLoss as shown on the scale in the figure inset.

A “Bra-ket” notations for probability formulas

This appendix introduces a convenient mathematical representation of probability distribution functions and of conditional density functions using notations involving bra-vector and ket-vector, according to the following definition:

- 1a. A single ”bra-vector” $\langle A |$ means the unconditional probability for A .
- 1b. A single ”ket-vector” $|B\rangle$ indicates the conditions where event B is assumed to happen.
- 2a. Scalar-multiplication for “bra-vector” satisfies the commutative law: $k \cdot \langle A | = \langle A | \cdot k, k \in \mathbb{R}$
- 2b. Scalar-multiplication for “ket-vector” satisfies the commutative law: $k \cdot |B\rangle = |B\rangle \cdot k, k \in \mathbb{R}$
- 3 The multiplication between a single “bra” and a single “ket” vector makes a complete pair-wise bra-ket $\langle A | B \rangle$, which represents the conditional distribution $f(A | B)$. The bra-ket can be regarded as a number.
- 4a. The notation $|A\rangle\langle A|$ to concatenate a single “ket” vector and a single “bra” vector defines the operator to transform a “ket” (“bra”) into another “ket” (“bra”), which leads to
 - $\langle B | (|A\rangle\langle A |) = \langle B | A \rangle \langle A | = \langle BA |$
 - $(|A\rangle\langle A |) |B\rangle = |AB\rangle \cdot \langle A | B \rangle$
- 4b. Given $A = \bigcup_i A_i$, then $\sum_i |A_i\rangle\langle A_i| = |1\rangle\langle 1| := I$ where $I = |1\rangle\langle 1|$ denotes the identical operator such that $\langle B | (|1\rangle\langle 1 |) = (\langle B | 1 \rangle) \langle 1 | = f(B|1) \langle 1 |$, where 1 denotes the whole universe, and thus $\langle 1 | = p(1) = 1$ and $f(B|1) := f(B) = \langle B |$ so that $\langle B | (|1\rangle\langle 1 |) = \langle B |$.

Further, according to the previous defined notations, the classic conditional probability and Bayesian formula can be rewritten as

- **(Conditional probability formula):** $\langle A | B \rangle = \frac{\langle AB |}{\langle B |}$ or $\langle AB | = \langle A | B \rangle \langle B |$
- **(The Bayesian formula):** $\langle A | B \rangle = \langle A | \frac{\langle B | A \rangle}{\langle B |}$

With the listed formal rules and the basic formula, we can easily give the derivations for the following famous formula in probability theory.

1. *(The Law of Total probability):* $\langle A | = \langle A | I = \langle A | \cdot \sum_i |B_i\rangle\langle B_i| = \sum_i \langle A | B_i \rangle \langle B_i |$
2. *(Decomposed Conditional Joint Density):*

$$\begin{aligned} \langle A, B | C \rangle &= \langle AB | \cdot |C\rangle = (\langle A | B \rangle \langle B |) \cdot |C\rangle \\ &= \langle A | (|B\rangle\langle B |) |C\rangle = \langle A | \cdot |BC\rangle \langle B | C \rangle \\ &= \langle A | B, C \rangle \langle B | C \rangle \end{aligned}$$

3. *(Multivariate Bayesian Formula):*

$$\begin{aligned} \langle A | B, C \rangle &= \frac{\langle A | BC \rangle \langle B | C \rangle}{\langle B | C \rangle} = \frac{\langle A | (|B\rangle\langle B |) |C\rangle}{\langle B | C \rangle} \\ &= \frac{\langle AB | \cdot |C\rangle}{\langle B | C \rangle} = \frac{\langle BA | \cdot |C\rangle}{\langle B | C \rangle} = \frac{\langle B | (|A\rangle\langle A |) |C\rangle}{\langle B | C \rangle} \\ &= \langle A | C \rangle \frac{\langle B | A, C \rangle}{\langle B | C \rangle} \end{aligned}$$

B Proof of eq.(10)

Proof. Since $p_t^{-n} | p_{t-1}^{-n} \sim \mathcal{N}(p_{t-1}^{-n} - n\mu_1, n^2\sigma_1^2)$, one can get

$$\langle p_t^{-n} | p_{t-1}^{-n} \rangle = \frac{1}{\sqrt{2\pi}\sigma_1} \exp \left[-\frac{1}{2} \cdot \left(\frac{p_t^{-n} - p_{t-1}^{-n} - \mu_1}{\sigma_1} \right)^2 \right]. \quad (38)$$

With the density transformation formula $f_{\bar{x}|\bar{y}}(x|y) = f_{\bar{x}|\bar{y}}(\phi(x)|y)|\phi'(x)|$, or equivalently $\langle x | y \rangle = \langle \phi(x) | y \rangle \cdot |\phi'(x)|$, eq.(38) further leads to

$$\langle p_t | p_{t-1} \rangle = \frac{1}{\sqrt{2\pi} \cdot n\sigma_1} \exp \left[-\frac{1}{2} \cdot \left(\frac{p_t^{-n} - p_{t-1}^{-n} + n\mu_1}{n\sigma_1} \right)^2 \right] \cdot np_t^{-(n+1)} \quad (39)$$

From the definition $y_t = \ln p_t$, and using the density transformation formula again, we obtain

$$\langle y_t | y_{t-1} \rangle = \langle e^{y_t} | y_{t-1} \rangle e^{y_t} = \langle p_t | y_t \rangle p_t \quad (40)$$

$$= \frac{1}{\sqrt{2\pi} \cdot n\sigma_1} \exp \left[-\frac{1}{2} \cdot \left(\frac{e^{-ny_t} - e^{-ny_{t-1}} + n\mu_1}{n\sigma_1} \right)^2 \right] \cdot ne^{-ny_t} \quad (41)$$

Consequently, we have

$$\ln \langle y_t | 1, 1, y_{t-1} \rangle = -\frac{1}{2} \ln 2\pi - \ln n\sigma_1 - \frac{1}{2} \cdot \left(\frac{e^{-ny_t} - e^{-ny_{t-1}} + n\mu_1}{n\sigma_1} \right)^2 + \ln n - ny_t \quad (42)$$

□

C Derivations for the equations in EM algorithm

C.1 proof of the eq. (14) from eq.(13)

Proof.

$$\begin{aligned} \ln \mathcal{L}_{\theta | \theta^{(k-1)}} &= \sum_{1 \dots T} \ln \langle y_{-o}^T, s_{-o}^T | \theta \rangle \langle y_{-o}^T, s_{-o}^T | \theta^{(k-1)} \rangle = \sum_{1 \dots T} \ln(\langle y_{-o}^T | s_{-o}^T \rangle_{\theta} \langle s_{-o}^T | \theta \rangle) \langle y_{-o}^T, s_{-o}^T | \theta^{(k-1)} \rangle \\ &= \sum_{1 \dots T} \ln \langle y_{-o}^T | s_{-o}^T \rangle_{\theta} \langle y_{-o}^T, s_{-o}^T | \theta^{(k-1)} \rangle + \sum_{1 \dots T} \ln \langle s_{-o}^T | \theta \rangle \langle y_{-o}^T, s_{-o}^T | \theta^{(k-1)} \rangle \end{aligned} \quad (43)$$

For the first item in the r.h.s. of (43), we can further obtain

$$\begin{aligned} \sum_{1 \dots T} \ln \langle y_{-o}^T | s_{-o}^T \rangle_{\theta} \langle y_{-o}^T, s_{-o}^T | \theta^{(k-1)} \rangle &= \sum_{1 \dots T} \left(\sum_{t=1}^T \ln \langle y_t | s_t, s_{t-1}, y_{-o}^{t-1} \rangle_{\theta} \right) \langle y_{-o}^T, s_{-o}^T | \theta^{(k-1)} \rangle \\ &= \sum_{t=1}^T \left(\sum_{t, t-1} \sum_{/t, /t-1} \ln \langle y_t | s_t, s_{t-1}, y_{-o}^{t-1} \rangle_{\theta} \langle y_{-o}^T, s_{-o}^T | \theta^{(k-1)} \rangle \right) \\ &= \sum_{t=1}^T \sum_{t, t-1} \left(\ln \langle y_t | s_t, s_{t-1}, y_{-o}^{t-1} \rangle_{\theta} \sum_{/t, /t-1} \langle y_{-o}^T, s_{-o}^T | \theta^{(k-1)} \rangle \right) \\ &= \sum_{t=1}^T \left(\sum_{t, t-1} \ln \langle y_t | s_t, s_{t-1}, y_{-o}^{t-1} \rangle_{\theta} \langle y_{-o}^T, s_t, s_{t-1} | \theta^{(k-1)} \rangle \right) \\ &= \langle y_{-o}^T | \theta^{(k-1)} \rangle \sum_{t=1}^T \left(\sum_{t, t-1} \ln \langle y_t | s_t, s_{t-1}, y_{-o}^{t-1} \rangle_{\theta} \langle s_{t-1}, s_t | y_{-o}^T \rangle_{\theta^{(k-1)}} \right) \end{aligned}$$

where the notation $\sum_{/t,/t-1}$ represents the summation for all states $s_\tau, \tau = 1, \dots, T$, except for s_{t-1} and s_t . The second term in the r.h.s. of (43) leads to

$$\begin{aligned}
\sum_{1 \dots T} \ln \langle s_{-o}^T | \boldsymbol{\theta} \rangle \langle y_{-o}^T, s_{-o}^T | \boldsymbol{\theta}^{(k-1)} \rangle &= \sum_{1 \dots T} \left(\sum_{t=1}^T \ln \langle s_t | s_{t-1} \rangle_{\boldsymbol{\theta}} \right) \langle y_{-o}^T, s_{-o}^T | \boldsymbol{\theta}^{(k-1)} \rangle \\
&= \sum_{t=1}^T \left(\sum_{/t,/t-1} \ln \langle s_t | s_{t-1} \rangle_{\boldsymbol{\theta}} \langle y_{-o}^T, s_{-o}^T | \boldsymbol{\theta}^{(k-1)} \rangle \right) \\
&= \sum_{t=1}^T \sum_{/t,/t-1} \left(\ln \langle s_t | s_{t-1} \rangle_{\boldsymbol{\theta}} \langle y_{-o}^T, s_{-o}^T | \boldsymbol{\theta}^{(k-1)} \rangle \right) \\
&= \langle y_{-o}^T | \boldsymbol{\theta}^{(k-1)} \rangle \sum_{t=1}^T \left(\sum_{/t,/t-1} \ln \langle s_t | s_{t-1} \rangle_{\boldsymbol{\theta}} \langle s_{t-1}, s_t | y_{-o}^T \rangle_{\boldsymbol{\theta}^{(k-1)}} \right)
\end{aligned}$$

Thus, we finally obtain (14)

$$\ln \mathcal{L}_{\boldsymbol{\theta}^{(k)} | \boldsymbol{\theta}^{(k-1)}} = \langle y_{-o}^T | \boldsymbol{\theta}^{(k-1)} \rangle \cdot \left(\sum_{t=1}^T \sum_{\substack{s_t=1,0 \\ s_{t-1}=1,0}} \left(\ln \langle y_t | s_t, s_{t-1}, y_{t-1} \rangle_{\boldsymbol{\theta}^{(k)}} + \ln \langle s_t | s_{t-1} \rangle_{\boldsymbol{\theta}^{(k)}} \right) \langle s_{t-1}, s_t | y_{-o}^T \rangle_{\boldsymbol{\theta}^{(k-1)}} \right)$$

□

C.2 Derivation of the formulas to determine the first four parameters of the HMM

Since $\langle s_{-o}^T | \boldsymbol{\theta}$ does not depend on $\boldsymbol{\theta} = (\mu_0, \sigma_0, \mu_1, \sigma_1, n)$, one can ignore the second term in eq. (43) when calibrating the parameters of the HMM.

In order to compute $\mu_0^{(k)}$, the first-order condition of the first term in eq. (43) reads

$$\sum_{t=1}^T \left(\sum_{\substack{s_t=1,0 \\ s_{t-1}=1,0}} \frac{\partial}{\partial \mu_0} \ln \langle y_t | s_t, s_{t-1}, y_{t-1} \rangle_{\boldsymbol{\theta}} \langle s_t, s_{t-1} | y_{-o}^T \rangle_{\boldsymbol{\theta}^{(k-1)}} \right) = 0 \quad (44)$$

which leads to

$$\begin{aligned}
&\sum_{t=1}^T \left(\frac{y_t - y_{t-1} - \mu_0}{\sigma_0} \langle s_t = 0, s_{t-1} = 0 | y_{-o}^T \rangle_{\boldsymbol{\theta}^{(k-1)}} \right) = 0 \\
\Rightarrow &\mu_0 = \frac{\sum_{t=1}^T (y_t - y_{t-1}) \langle s_t = 0, s_{t-1} = 0 | y_{-o}^T \rangle_{\boldsymbol{\theta}^{(k-1)}}}{\sum_{t=1}^T \langle s_t = 0, s_{t-1} = 0 | y_{-o}^T \rangle_{\boldsymbol{\theta}^{(k-1)}}} \\
\Rightarrow &\mu_0^{(k)} = \frac{\sum_{t=1}^T \omega_{(0,0);t}^{(k-1)} (y_t - y_{t-1})}{\sum_{t=1}^T \omega_{(0,0);t}^{(k-1)}}
\end{aligned}$$

In order to compute $\sigma_0^{(k)}$, the first-order condition of the first term in eq. (43) reads

$$\sum_{t=1}^T \left(\sum_{\substack{s_t=1,0 \\ s_{t-1}=1,0}} \frac{\partial}{\partial \sigma_0} \ln \langle y_t | s_t, s_{t-1}, y_{t-1} \rangle_{\boldsymbol{\theta}} \langle s_t, s_{t-1} | y_{-o}^T \rangle_{\boldsymbol{\theta}^{(k-1)}} \right) = 0 \quad (45)$$

which leads to

$$\begin{aligned} \sum_{t=1}^T \left(-\frac{1}{\sigma_0} + \frac{(y_t - y_{t-1} - \mu_0)^2}{\sigma_0^3} \right) \langle s_t = 0, s_{t-1} = 0 \mid y_{-\infty}^T \rangle_{\boldsymbol{\theta}^{(k-1)}} &= 0 \\ \Rightarrow \sigma_0^{(k)} &= \sqrt{\frac{\sum_{t=1}^T \omega_{(0,0);t}^{(k-1)} (y_t - y_{t-1} - \mu_0^{(k)})^2}{\sum_{t=1}^T \omega_{(0,0);t}^{(k-1)}}} \end{aligned}$$

In order to compute $\mu_1^{(k)}$, the first-order condition of the first term in eq. (43) reads

$$\sum_{t=1}^T \left(\sum_{\substack{s_t=1,0 \\ s_{t-1}=1,0}} \frac{\partial}{\partial \mu_1} \ln \langle y_t \mid s_t, s_{t-1}, y_{t-1} \rangle_{\boldsymbol{\theta}} \langle s_t, s_{t-1} \mid y_{-\infty}^T \rangle_{\boldsymbol{\theta}^{(k-1)}} \right) = 0 \quad (46)$$

which leads to

$$\begin{aligned} \sum_{t=1}^T \left(-\frac{p_t^{-n} - p_{t-1}^{-n} + n\mu_1}{n\sigma_1^2} \right) \langle s_t = 1, s_{t-1} = 1 \mid y_{-\infty}^T \rangle_{\boldsymbol{\theta}^{(k-1)}} &= 0 \\ \Rightarrow \sum_{t=1}^T (-p_t^{-n} + p_{t-1}^{-n} - n\mu_1) \omega_{(1,1);t}^{(k-1)} &= 0 \\ \Rightarrow \mu_1^{(k)} &= \frac{\sum_{t=1}^T \omega_{(1,1);t}^{(k-1)} (p_{t-1}^{-n} - p_t^{-n})}{n \sum_{t=1}^T \omega_{(1,1);t}^{(k-1)}} \end{aligned}$$

In order to compute $\sigma_1^{(k)}$, the first-order condition of the first term in eq. (43) reads

$$\sum_{t=1}^T \left(\sum_{\substack{s_t=1,0 \\ s_{t-1}=1,0}} \frac{\partial}{\partial \sigma_1} \ln \langle y_t \mid s_t, s_{t-1}, y_{t-1} \rangle_{\boldsymbol{\theta}} \langle s_t, s_{t-1} \mid y_{-\infty}^T \rangle_{\boldsymbol{\theta}^{(k-1)}} \right) = 0 \quad (47)$$

which leads to

$$\begin{aligned} \sum_{t=1}^T \left(\frac{1}{\sigma_1} - \frac{(p_t^{-n} - p_{t-1}^{-n} + n\mu_1)^2}{n^2 \sigma_1^3} \right) \langle s_t = 1, s_{t-1} = 1 \mid y_{-\infty}^T \rangle_{\boldsymbol{\theta}^{(k-1)}} &= 0 \\ \Rightarrow \sum_{t=1}^T [(p_t^{-n} - p_{t-1}^{-n} + n\mu_1)^2 - n^2 \sigma_1^2] \omega_{(1,1);t}^{(k-1)} &= 0 \\ \Rightarrow \sigma_1^{(k)} &= \sqrt{\frac{\sum_{t=1}^T \omega_{(1,1);t}^{(k-1)} (p_t^{-n} - p_{t-1}^{-n} + n\mu_1^{(k)})^2}{n^2 \sum_{t=1}^T \omega_{(1,1);t}^{(k-1)}}} \end{aligned}$$

C.3 Derivation for eq.(15) to solve for n

To compute $n^{(k)}$, one should solve the first-order condition of the first term in eq. (43) with respect to n , that is

$$\sum_{t=1}^T \left(\sum_{\substack{s_t=1,0 \\ s_{t-1}=1,0}} \frac{\partial}{\partial n} \ln \langle y_t \mid s_t, s_{t-1}, y_{t-1} \rangle_{\boldsymbol{\theta}} \langle s_t, s_{t-1} \mid y_{-\infty}^T \rangle_{\boldsymbol{\theta}^{(k-1)}} \right) = 0 \quad (48)$$

which gives,

$$\sum_{t=1}^T \left(-\frac{(p_t^{-n} - p_{t-1}^{-n} + n\mu_1)(-p_t^{-n} \ln p_t + p_{t-1}^{-n} \ln p_{t-1} + \mu_1)}{n^2 \sigma_1^2} + \frac{(p_t^{-n} - p_{t-1}^{-n} + n\mu_1)^2}{n^3 \sigma_1^2} - \frac{1}{n} + \frac{1}{n} - \ln p_t \right) \omega_{(1,1):t}^{(k-1)} = 0 \quad (49)$$

Note that $\sum_{t=1}^T \left(\frac{(p_t^{-n} - p_{t-1}^{-n} + n\mu_1)^2}{n^3 \sigma_1^2} - \frac{1}{n} \right) \omega_{(1,1):t}^{(k-1)} = 0$. Thus, the above equation can be reduced to

$$\sum_{t=1}^T \left(-\frac{(p_t^{-n} - p_{t-1}^{-n} + n\mu_1)(-p_t^{-n} \ln p_t + p_{t-1}^{-n} \ln p_{t-1} + \mu_1)}{n^2 \sigma_1^2} + \frac{1}{n} - \ln p_t \right) \omega_{(1,1):t}^{(k-1)} = 0 \quad (50)$$

C.4 Derivation of the formulas to compute the optimal posterior transition probability from s_{t-1} to s_t

Since $\langle s_t | s_{t-1} \rangle_{\theta^{(k)}}$ is only related to the second term in eq.(43), we can ignore the first term when performing the optimization:

$$\begin{aligned} \sum_{1 \dots T} \ln \langle s_{-}^T | \theta \rangle_{\langle y_{-}^T, s_{-}^T | \theta^{(k-1)} \rangle} &= \sum_{t=1}^T \left(\sum_{t,t-1} \ln \langle s_t | s_{t-1} \rangle_{\theta} \langle s_t, s_{t-1} | y_{-}^T \rangle_{\theta^{(k-1)}} \right) \\ &= \sum_{t=1}^T \left(\sum_{j,i} \ln q_{ij}^{(k)} \langle j, i | y_{-}^T \rangle_{\theta^{(k-1)}} \right) \end{aligned}$$

Without loss of generality, the first-order condition against q_{i1} leads to

$$\begin{aligned} 0 &= \sum_{t=1}^T \left(\frac{\partial}{\partial q_{i1}^{(k)}} \ln q_{ij}^{(k)} \langle i, j | y_{-}^T \rangle_{\theta^{(k-1)}} \right) \\ &= \sum_{t=1}^T \left(\frac{1}{q_{i1}^{(k)}} \langle 1, i | y_{-}^T \rangle_{\theta^{(k-1)}} - \frac{1}{1 - q_{i1}^{(k)}} \langle 0, i | y_{-}^T \rangle_{\theta^{(k-1)}} \right) \end{aligned}$$

Then we have

$$q_{i1}^{(k)} = \frac{\sum_{t=1}^T \langle 1, i | y_{-}^T \rangle_{\theta^{(k-1)}}}{\sum_{t=1}^T (\langle 1, i | y_{-}^T \rangle_{\theta^{(k-1)}} + \langle 0, i | y_{-}^T \rangle_{\theta^{(k-1)}})} = \frac{\sum_{t=1}^T \langle 1, i | y_{-}^T \rangle_{\theta^{(k-1)}}}{\sum_{t=1}^T \langle i | y_{-}^T \rangle_{\theta^{(k-1)}}}$$

It is the optimal posterior transition probability after the k th iteration, $q_{ij}^{(k)}$, when $j = 1$.

C.5 Reasoning to replace $\langle s_t \mid s_{t+1}, y_{-o}^t, y_{t+1}^- \rangle$ by $\langle s_t \mid s_{t+1}, y_{-o}^t \rangle$ in eq.(20)

$$\langle s_t \mid s_{t+1}, y_{-o}^t, y_{t+1}^- \rangle = \frac{\langle s_t \mid \left(\mid s_{t+1}, y_{-o}^t, y_{t+1}^- \rangle \right) \langle y_{t+1}^- \mid s_{t+1}, y_{-o}^t \rangle}{\langle y_{t+1}^- \mid s_{t+1}, y_{-o}^t \rangle} \quad (51)$$

$$= \frac{\langle s_t \mid \left(\mid s_{t+1}, y_{-o}^t, y_{t+1}^- \rangle \langle y_{t+1}^- \mid s_{t+1}, y_{-o}^t \rangle \right)}{\langle y_{t+1}^- \mid s_{t+1}, y_{-o}^t \rangle} \quad (52)$$

$$= \frac{\langle s_t \mid \left(\mid y_{t+1}^- \rangle \langle y_{t+1}^- \mid \right) \mid s_{t+1}, y_{-o}^t \rangle}{\langle y_{t+1}^- \mid s_{t+1}, y_{-o}^t \rangle} \quad (53)$$

$$= \frac{\left(\langle s_t \mid y_{t+1}^- \rangle \langle y_{t+1}^- \mid \right) \mid s_{t+1}, y_{-o}^t \rangle}{\langle y_{t+1}^- \mid s_{t+1}, y_{-o}^t \rangle} = \frac{\langle y_{t+1}^- \mid \left(\mid s_t \rangle \langle s_t \mid \right) \mid s_{t+1}, y_{-o}^t \rangle}{\langle y_{t+1}^- \mid s_{t+1}, y_{-o}^t \rangle} \quad (54)$$

$$= \frac{\langle y_{t+1}^- \mid s_t, s_{t+1}, y_{-o}^t \rangle \langle s_t \mid s_{t+1}, y_{-o}^t \rangle}{\langle y_{t+1}^- \mid s_{t+1}, y_{-o}^t \rangle} \quad (55)$$

By assuming that the joint distribution of $(y_{t+1}, y_{t+2}, \dots, y_T)$ is irrelevant to s_t , we can eliminate the denominator and easily recover (55) for $\langle s_t \mid s_{t+1}, y_{-o}^t \rangle$

References

- Andersen, J., Sornette, D., 2004. Fearless versus fearful speculative financial bubbles. *Physica A: Statistical Mechanics and its Applications* 337 (3-4), 565–585.
- Ardila-Alvarez, D., Forró, Z., Sornette, D., 2015. The acceleration effect and gamma factor in asset pricing. Swiss Finance Institute Research Paper No. 15-30. Available at SSRN: <http://ssrn.com/abstract=2645882>.
- Avery, C., Zemsky, P., 1998. Multidimensional uncertainty and herd behavior in financial markets. *American Economic Review* 88 (4), 724–748.
- Banerjee, A. V., 1992. A simple model of herd behavior. *The Quarterly Journal of Economics* 107 (3), 797–817.
- Barberis, N., Shleifer, A., Vishny, R., 1998. A model of investor sentiment. *Journal of Financial Economics* 49 (3), 307–343.
- Barnett, L., Barrett, A. B., Seth, A. K., 2009. Granger causality and transfer entropy are equivalent for Gaussian variables. *Physical Review Letters* 103 (23), 238701.
- Barrett, A. B., Barnett, L., 2013. Granger causality is designed to measure effect, not mechanism. *Frontiers in Neuroinformatics* 7 (6), 1–2.
- Bikhchandani, S., Hirshleifer, D., Welch, I., 1992. A theory of fads, fashion, custom, and cultural change as informational cascades. *Journal of Political Economy* 100 (5), 992–1026.
- Brunnermeier, M. K., Oehmke, M., 2013. Bubbles, financial crises, and systemic risk. *Handbook of the Economics of Finance*. Amsterdam: Elsevier 2 (B), 1221–1288.
- Cajueiro, D., Tabak, B., Werneck, F., 2009. Can we predict crashes? The case of the Brazilian stock market. *Physica A: Statistical Mechanics and its Applications* 388 (8), 1603–1609.
- Chiang, T. C., Li, J., Tan, L., 2010. Empirical investigation of herding behavior in chinese stock markets: Evidence from quantile regression analysis. *Global Finance Journal* 21 (1), 111–124.
- Chincarini, L. B., 2012. *The Crisis of Crowding: Quant Copycats, Ugly Models, and the New Crash Normal*. John Wiley & Sons.
- Choi, N., Sias, R. W., 2009. Institutional industry herding. *Journal of Financial Economics* 94 (3), 469–491.
- Dass, N., Massa, M., Patgiri, R., 2008. Mutual funds and bubbles: The surprising role of contractual incentives. *Review of Financial Studies* 21 (1), 51–99.
- Dempster, A. P., Laird, N. M., Rubin, D. B., 1977. Maximum likelihood from incomplete data via the EM algorithm. *Journal of the Royal Statistical Society. Series B (Methodological)* 39 (1), 1–38.
- Devenow, A., Welch, I., 1996. Rational herding in financial economics. *European Economic Review* 40 (3), 603–615.
- Dimitriadi, G., 2004. What are "financial bubbles": Approaches and definitions. *Electronic Journal "INVESTIGATED in RUSSIA"*.

- Filimonov, V., Sornette, D., 2013. A stable and robust calibration scheme of the log-periodic power law model. *Physica A-Statistical Mechanics and Its Applications* 392 (17), 3698–3707.
- Giordano, M., Mannella, R., 2006. A brief analysis of may 2004 crash in the indian market. *Fluctuation and Noise Letters* 6 (3), 243–249.
- Gurkaynak, R. S., 2008. Econometric tests of asset price bubbles: taking stock. *Journal of Economic Surveys* 22 (1), 166–186.
- Hamilton, J. D., 1989. A new approach to the economic analysis of nonstationary time series and the business cycle. *Econometrica: Journal of the Econometric Society* 57 (2), 357–384.
- He, Z., Su, D., 2009. Price manipulation and industry momentum: Evidence from the chinese stock market. Available at SSRN: <http://ssrn.com/abstract=1393505>.
- Hlaváčková-Schindler, K., 2011. Equivalence of granger causality and transfer entropy: a generalization. *Applied Mathematical Sciences* 5 (73), 3637–3648.
- Hong, H., Kubik, J. D., Stein, J. C., 2005. Thy neighbor's portfolio: Word-of-mouth effects in the holdings and trades of money managers. *Journal of Finance* 60 (6), 2801–2824.
- Hüsler, A., Sornette, D., Hommes, C. H., 2013. Super-exponential bubbles in lab experiments: evidence for anchoring over-optimistic expectations on price. *Journal Economic Behavior and Organization* 92, 304–316.
- Ide, K., Sornette, D., 2002. Oscillatory finite-time singularities in finance, population and rupture. *Physica A* 307 (1-2), 63–106.
- Jeanblanc, M., Yor, M., Chesney, M., 2009. *Mathematical Methods for Financial Markets*. Springer Finance, Springer Finance Textbooks.
- Jiang, Z.-Q., Zhou, W.-X., Sornette, D., Woodard, R., Bastiaensen, K., Cauwels, P., 2010. Bubble diagnosis and prediction of the 2005-2007 and 2008-2009 chinese stock market bubbles. *Journal of Economic Behavior & Organization* 74 (3), 149–162.
- Johansen, A., Ledoit, O., Sornette, D., 2000. Crashes as critical points. *International Journal of Theoretical and Applied Finance* 3, 219–255.
- Johansen, A., Sornette, D., 2000. The nasdaq crash of april 2000: Yet another example of log-periodicity in a speculative bubble ending in a crash. *European Physical Journal B* 17, 319–328.
- Johansen, A., Sornette, D., 2001. Bubbles and anti-bubbles in latin-american, asian and western stock markets: an empirical study. *International Journal of Theoretical and Applied Finance* 4 (6), 853–920.
- Johansen, A., Sornette, D., Ledoit, O., 1999. Predicting financial crashes using discrete scale invariance. *Journal of Risk* 1 (4), 5–32.
- Kaizoji, T., Leiss, M., Saichev, A., Sornette, D., 2015. Super-exponential endogenous bubbles in an equilibrium model of rational and noise traders. *Journal of Economic Behavior and Organization* 112, 289–310.
- Khwaja, A. I., Mian, A., 2005. Unchecked intermediaries: Price manipulation in an emerging stock market. *Journal of Financial Economics* 78 (1), 203–241.

- Kim, C.-J., Nelson, C. R., 1999. State-space models with regime switching. Cambridge, Mass.
- Lakonishok, J., Shleifer, A., Vishny, R. W., 1994. Contrarian investment, extrapolation, and risk. *The Journal of Finance* 49 (5), 1541–1578.
- Leiss, M., Nax, H., Sornette, D., 2015. Super-exponential growth expectations and the global financial crisis. *Journal of Economic Dynamics and Control* 55, 1–13.
- Li, W., Rhee, G., Wang, S. S., 2009. Differences in herding: individual vs. institutional investors in china. *Institutional Investors in China* (SSRN: February 13, 2009).
- Lin, L., Ren, R.-E., Sornette, D., 2014. The volatility-confined LPPL model: A consistent model of ‘explosive’ financial bubbles with mean-reverting residuals. *International Review of Financial Analysis* 33, 210–225.
- Lin, L., Sornette, D., 2013. Diagnostics of rational expectation financial bubbles with stochastic mean-reverting termination times. *The European Journal of Finance* 19 (5), 344–365.
- Long, J. B. D., Shleifer, A., Summers, L. H., Waldmann, R. J., 1990. Noise trader risk in financial markets. *Journal of Political Economy* 98 (4), 703–738.
- Matsushita, R., da Silva, S., Figueiredo, A., Gleria, I., 2006. Log-periodic crashes revisited. *Physica A: Statistical Mechanics and its Applications* 364, 331–335.
- Nofsinger, J. R., Sias, R. W., 1999. Herding and feedback trading by institutional and individual investors. *The Journal of Finance* 54 (6), 2263–2295.
- Piotroski, J. D., Wong, T., 2011. Institutions and information environment of chinese listed firms. In: *Capitalizing China*. University of Chicago Press, pp. 201–242.
- Redner, S., 2001. *A Guide to First-Passage Processes*. Cambridge University Press.
- Roehner, B. M., Sornette, D., 2000. “Thermometers” of speculative frenzy. *The European Physical Journal B-Condensed Matter* 16 (4), 729–739.
- Shiller, R. J., 2000. *Irrational exuberance*. Princeton University Press, NJ.
- Sias, R. W., 2004. Institutional herding. *Review of Financial Studies* 17 (1), 165–206.
- Sornette, D., 1998. Discrete-scale invariance and complex dimensions. *Physics Reports* 297, 239–270.
- Sornette, D., Andersen, J. V., 2002. A nonlinear super-exponential rational model of speculative financial bubbles. *International Journal of Modern Physics C* 13 (2), 171–188.
- Sornette, D., Cauwels, P., 2014. 1980-2008: The illusion of the perpetual money machine and what it bodes for the future. *Risks* 2, 103–131.
- Sornette, D., Cauwels, P., 2015. Financial bubbles: mechanisms and diagnostics. *Review of Behavioral Economics* 2 (3), <http://ssrn.com/abstract=2423790>.
- Sornette, D., Demos, G., Zhang, Q., Cauwels, P., Filimonov, V., Zhang, Q., 2015. Real-time prediction and post-mortem analysis of the Shanghai 2015 stock market bubble and crash. *Journal of Investment Strategies* 4 (4), 77–95.

- Sornette, D., Johansen, A., 1998. A hierarchical model of financial crashes. *Physica A: Statistical Mechanics and Its Applications-Statistical Mechanics and Its Applications* 261, 581–598.
- Sornette, D., Woodard, R., 2010. Financial bubbles, real estate bubbles, derivative bubbles, and the financial and economic crisis. *Proceedings of APFA7 (Applications of Physics in Financial Analysis)*, “New Approaches to the Analysis of Large-Scale Business and Economic Data,” Misako Takayasu, Tsutomu Watanabe and Hideki Takayasu, eds., Springer, <http://arxiv.org/abs/0905.0220>.
- Sornette, D., Woodard, R., Zhou, W. X., 2009. The 2006–2008 oil bubble: Evidence of speculation, and prediction. *Physica A: Statistical Mechanics and its Applications* 388, 1571–1576.
- Sornette, D., Zhou, W.-X., 2006. Predictability of large future changes in major financial indices. *International Journal of Forecasting* 22, 153–168.
- Tan, L., Chiang, T. C., Mason, J. R., Nelling, E., 2008. Herding behavior in chinese stock markets: An examination of a and b shares. *Pacific-Basin Finance Journal* 16 (1), 61–77.
- Xu, N.-X., Yu, S.-R., Yin, Z. H., 2013. Institutional investor herding and stock price crash risk. *Management World (Chinese)* (7), 31–43.
- Zhou, C.-S., Yang, Y. H., Wang, Y.-P., 2005. Trading-based market manipulation in china’s stock market. *Economic Research Journal (In Chinese)* 10.
- Zhou, W. X., Sornette, D., 2006a. Fundamental factors versus herding in the 2000-2005 us stock market and prediction. *Physica A: Statistical Mechanics and Its Applications* 360 (2), 459–482.
- Zhou, W. X., Sornette, D., 2006b. Is there a real-estate bubble in the us? *Physica A-Statistical Mechanics and Its Applications* 361 (1), 297–308.
- Zhou, W.-X., Sornette, D., 2008. Analysis of the real estate market in las vegas: Bubble, seasonal patterns, and prediction of the csw indexes. *Physica A: Statistical Mechanics and its Applications* 387, 243–260.
- Zhou, W.-X., Sornette, D., 2009. A case study of speculative financial bubbles in the South African stock market 2003-2006. *Physica A: Statistical Mechanics and its Applications* 388, 869–880.